metals

MDPI

Review

Investigating the Tribocorrosion Behaviour of NiTiNOL60 Alloy in Engineering and Biomedical Applications—An Overview

Anthony O. Okoani [1,2], Ashveen Nand [3], Cho-Pei Jiang [4] and Maziar Ramezani [1,*]

[1] Department of Mechanical Engineering, Auckland University of Technology, Auckland 1010, New Zealand; anthony.okoani@aut.ac.nz
[2] Department of Mechanical Engineering, University of Nigeria, Nsukka 410001, Nigeria
[3] Faculty of Engineering, University of Auckland, Auckland 1010, New Zealand; ashveen.nand@auckland.ac.nz
[4] Department of Mechanical Engineering, National Taipei University of Technology, Taipei 10608, Taiwan; jcp@mail.ntut.edu.tw
* Correspondence: maziar.ramezani@aut.ac.nz

Abstract: This review covers the literature that is currently accessible, as well as emerging research into the performance of NiTi-based alloys exposed to corrosive environments in both engineering and medical applications. It provides an overview of the state-of-the-art research in the study of tribocorrosion of Ni-rich NiTi alloy by highlighting significant discoveries, research approaches, and future research directions following the limited reviews on tribocorrosion in the past decade. The practical impacts, as well as the economic implications of tribological applications on daily life, coupled with the increasing failures of metals and biomaterials, make it imperative to investigate tribocorrosion and update the subject area on the recent focus. Tribocorrosion is commonly observed on the surface of different metals, including NiTi alloys, such as NiTiNOL60 (60 wt.% Ni and 40 wt.% Ti), which possess unique properties applicable across various engineering and biomedical fields. In its application, the material experiences wear due to the depassivation of tribofilms caused by relative motion (sliding, fretting, or impact) in aggressive environments, including corrosive mediums, high temperatures, and pressures. This study elucidates the synergistic interactions between mechanical wear, corrosion, and their associated tribocorrosion mechanisms in corrosive media.

Keywords: NiTiNOL60 alloy; biocompatibility; electrochemistry; tribocorrosion; wear

Citation: Okoani, A.O.; Nand, A.; Jiang, C.-P.; Ramezani, M. Investigating the Tribocorrosion Behaviour of NiTiNOL60 Alloy in Engineering and Biomedical Applications—An Overview. *Metals* **2024**, *14*, 1334. https://doi.org/10.3390/met14121334

Academic Editor: Branimir N. Grgur

Received: 15 October 2024
Revised: 17 November 2024
Accepted: 18 November 2024
Published: 25 November 2024

1. Introduction

The demand for a better understanding of surface degradation processes, mainly when tribological components are operating in corrosive environments, has arisen because of the need to choose or design new surfaces for future equipment, minimise operating costs, and extend the life of existing machinery [1,2]. This has led to the current study field of tribocorrosion, which aims to address the aforementioned issues and understand the mechanisms of surface deterioration when mechanical wear and chemical/electrochemical processes combine [3–5]. Tribocorrosion is a multifaceted degradation phenomenon that occurs when metals are subjected to mechanical wear and corrosion simultaneously [6–8].

The interaction between moving surfaces in a tribological loading situation/contact is a concept that exists in many phenomena in nature, be it in the components of spacecraft [9], human joints [10], rolling elements of a jet turbine [11], etc. The literature states that tribological contacts result in a global economic loss of approximately USD 300 billion annually, with friction contributing to 73% of the total loss and wear contributing to 27% [12]. Corrosion is also reported to have a global estimated cost of about USD 2.5 trillion, equivalent to 3.4% of the 2013 Gross Domestic Product of the United States [13]. Tribological applications in a corrosive environment often result in a surface alteration [14–16], and understanding this complex phenomenon and its complexity arises from the interactions involved in moving surfaces, as influenced by several parameters (mechanical, material, electrochemical

reaction, and environment) [5,6,8]. The interaction is a significant mechanism of degradation that has a big impact on the effectiveness and dependability of metallic materials. As such, superalloys are preferred over conventional materials in high service temperatures (650 °C) and other tribological operations [17–19] where the structural component may fail due to creep and/or fatigue.

This phenomenon, characterised by its synergy from the combined action of mechanical loading and corrosion attack influenced by the environment [20,21], is known as tribocorrosion. Its occurrence still prevails as the primary mechanism governing the deterioration of material through the interaction of wear and corrosion in numerous applications such as marine engineering [22,23], biomedical implants [24,25], aerospace [9,17], and chemical mechanical polishing [26]. In these applications, several phenomena, including abrasive wear, adhesive wear, corrosive wear, fretting corrosion, galvanic corrosion, and pitting corrosion, take place simultaneously, which can shorten the useful life of equipment/components, leading to unpredicted failures [5,27,28]. Different materials have been considered to remedy the situation; thus, steels are the most highly utilised engineering alloys due to their desirable properties of high tensile strength and good machinability [29]. For manufacturing implants, stainless steels are considered for their remarkably high-temperature resistance and performance against corrosive media. Still, their high wear resistance makes them unsuitable in high-temperature and load-bearing applications [25]. Low-carbon steels are also unsuitable, because they are susceptible to aqueous corrosion [30]. López-Ortega et al. [31] reported that the tribocorrosion of passive materials like stainless steel and titanium alloys has been widely studied for different applications and corrosive environments in recent decades. They highlighted that wear locally destroys and removes the protective oxide layer formed on the surface of passive materials, which exposes the underlying fresh material to the electrolyte [31]. Another study by Shabalovskaya et al. [32] highlights the potential threat of metallic release from implant devices and the subsequent research focus on surface modifications and coatings [33–35]. This has been a significant area of research due to the potential health risks associated with metallic exposure [36,37].

Another area of interest is the application of graphene and graphene oxide additives as barrier coatings in tribological applications due to their remarkable thermal conductivity, excellent mechanical strength, and high surface area, as well as weak van der Waals interactions between adjacent atomic-thick lamellae [38]. It has been reported that graphene-based materials used as additives to water and lubricating oils have significantly improved friction reduction, the protection of contact interfaces against wear, and corrosion mitigation through thin film formation [38,39]. Kumar et al. [39] highlighted the relevance of graphene barrier coatings and categorised the commonly used graphene-based anti-corrosion into pure graphene and graphene composite coatings. However, the dispersion stability, structural features, and dosage of graphene-based dispersoids, along with contact geometry, play important roles in governing tribological properties [38]. Accordingly, Zuo et al. [40] investigated the effect of various concentrations and tribocorrosion behaviour of graphene oxide (GO) particles in micro-arc oxidation (MAO) coating on the Ti6AL4V alloy. Their study confirmed that the GO additive effectively enhanced the corrosion/tribocorrosion resistance of MAO coatings and further reported that the best tribocorrosion resistance was achieved by combining MAO coating and 10 mL/L of GO [40]. Another study by Acar et al. [41] investigated boron-doped and graphene oxide-doped TiO_2 nanotubes (TNTs). Their study reported that the graphene oxide-doped TNT sample had the highest corrosion resistance and surface hardness, showing the best tribocorrosion resistance.

Since the lifespan of most engineering and biomedical materials is often affected by corrosion and sliding wear properties [5,36,42–46], it has prompted the growing interest and investigation for a suitable material that can withstand the synergistic impact of wear and corrosion [35,47]. Accordingly, researchers have explored nickel and titanium as significant elements mostly used in high-temperature applications [17–19,48–50]. These elements have superior oxidation and corrosion resistance with excellent stable mechanical properties at

higher service temperatures [51]. NiTiNOL60 alloy has been widely adopted in tribological applications due to its unique properties, such as high hardness, high corrosion resistance, low elastic modulus, and non-magnetic properties [52,53]. This alloy's high mechanical and corrosion resistance properties promote its application in harsh/aggressive environments, including marine [23] and biomedical implants [54]. Despite the excellent corrosion resistance property of NiTiNOL60 alloy, tribocorrosion still prevails as the primary mechanism governing the deterioration of material through the interaction of wear and corrosion in many engineering applications, such as marine engineering [22,23,55], biomedical implants [24], aerospace [9,17,56], and chemical mechanical polishing [26]. Aside from the aerospace, marine, and biomedical applications, Mathew et al. [57] listed the automotive, food and textile, chemical and oil industries, mining and metallurgy, thin films, micro- and nanotechnology coating, and the transportation industry as additional sectors where tribocorrosion synergy occurs.

Although NiTi alloys produced by traditional methods such as casting, wrought, etc. were the focus of many studies on tribocorrosion, the tribocorrosion characterisation of NiTi alloys produced by additive manufacturing processes is a relatively new and less explored topic in the literature [58,59]. As a result, Buciumeanu et al. [60] investigated the synergistic effects of corrosion and wear in phosphate-buffered saline on as-printed NiTi shape-memory alloy processed by additive manufacturing laser beam-directed energy deposition (LB-DED) techniques such as laser-engineered net shaping (LENS). They further compared the tribocorrosion behaviour of NiTi alloy with Ti-6Al-4V, the most commonly used titanium alloy in biomedical applications, produced using the same processing technology (LB-DED and LENS). Their study found that, when compared to the Ti-6Al-4V alloy [61], the NiTi alloy is less vulnerable to the discharge of metallic ions [37] during its service life as an implant [60,62]. NiTi shape-memory alloys possess several multifunctional properties resulting from a reversible martensitic transformation. Further studies showed that understanding the effects of specific parameters such as transformation temperatures, matrix strength, hysteresis, and transformation strain of NiTi alloys, which are functions of composition, thermomechanical treatment, and crystallographic orientation, is crucial for practical purposes [52,63,64]. This study has shown the need for a more recent review of the tribocorrosion of NiTi alloy. Accordingly, Mischler and Munoz [6] summarised the aspects of tribocorrosion studied at the time of their report. The information revealed that some areas have received little attention, and the fact that the combined actions of tribology and electrochemical reactions impact various activities makes this review relevant. Therefore, this paper provides a comprehensive review of the tribocorrosion behaviour of NiTiNOL60 alloy in corrosive environments, focusing on understanding the interactions between mechanical wear, corrosion, and the associated degradation mechanisms. Examining the experimental findings and research advancements will help unravel the performance of NiTi alloy under simultaneous mechanical and electrochemical stresses in tribological and corrosive conditions. Further, it tends to critically analyse the recent status of NiTi alloy tribocorrosion and highlight the future areas to be investigated to aid in the selection and application of NiTiNOL60 alloy.

2. NiTi-Based Alloys and the Fundamental Concepts in Tribology and Corrosion

2.1. NiTi Alloys

The need to create engineering systems that are more durable and long-lasting presents new and emerging issues for tribological interfaces. In that quest, Arne Ölander, in 1932, discovered the first smart alloy, referred to as the shape-memory alloy (SMA), suitable for different industrial fields [65]. It was acknowledged that the material's "shape-memory effect" showed improved recovery after a significant degree of strain and could replicate their memorised shapes [51]. In 1962, William J. Buehler and Fredrick Wang discovered NiTi alloy at the Naval Ordnance Laboratory (NOL), Ohio, USA, thus the name NiTiNOL [11,66,67]. Other thermomechanical characteristics of NiTiNOL, such as pseudoelasticity or high damping, were discovered later [65]. Since then, several metallic alloys with intrinsic

physical, mechanical, and electrical properties, including shape-memory behaviour, have been utilised in various industrial applications.

Figure 1 presents a nearly stoichiometric NiTi alloy phase equilibrium diagram; the transformation from B2 → B19′ occurs in a single step. In austenite, big grains (~6.6 to 21.7 μm) undergo the same transformation but with a relatively small Ni advantage. Grain development is the direct outcome of heating to a relatively high temperature of >800 °C, which also causes uneven release of the metastable Ni_4Ti_3 phase [68]. As the diagram illustrates, Ni_3Ti is the cuboid-shaped γ′ phase (hard-ordered phase) responsible for increasing the operating temperature of the SMA. At high and low temperatures, the stress-induced superelasticity and thermally induced shape-memory effect aid SMAs' recovery of their original shapes [69]. Patel and Bahera examined the triangular region of the NiTi phase diagram in their work, and they emphasised the combined influence of SMA and superalloy qualities based on the phases that occurred [51]. In another study, Dobrzański et al. [68] investigated the effect of a mass concentration of nickel in the range of 48–51% on the martensite start (M_s) temperature value. They deduced that the M_s temperature for the stoichiometric chemical composition of Ni50–Ti50 is around 65 °C. This temperature also slightly increases with the increasing titanium content. Conversely, when the nickel concentration is increased above equilibrium, the M_s temperature is drastically lowered to around 140 °C [68]. Therefore, it is possible to express the series of precipitation processes in austenite with structure B2 systematically depleted in alloying elements under such circumstances as B2 → Ti_3Ni_4 → Ti_2Ni_3 → $TiNi_3$ [68,69].

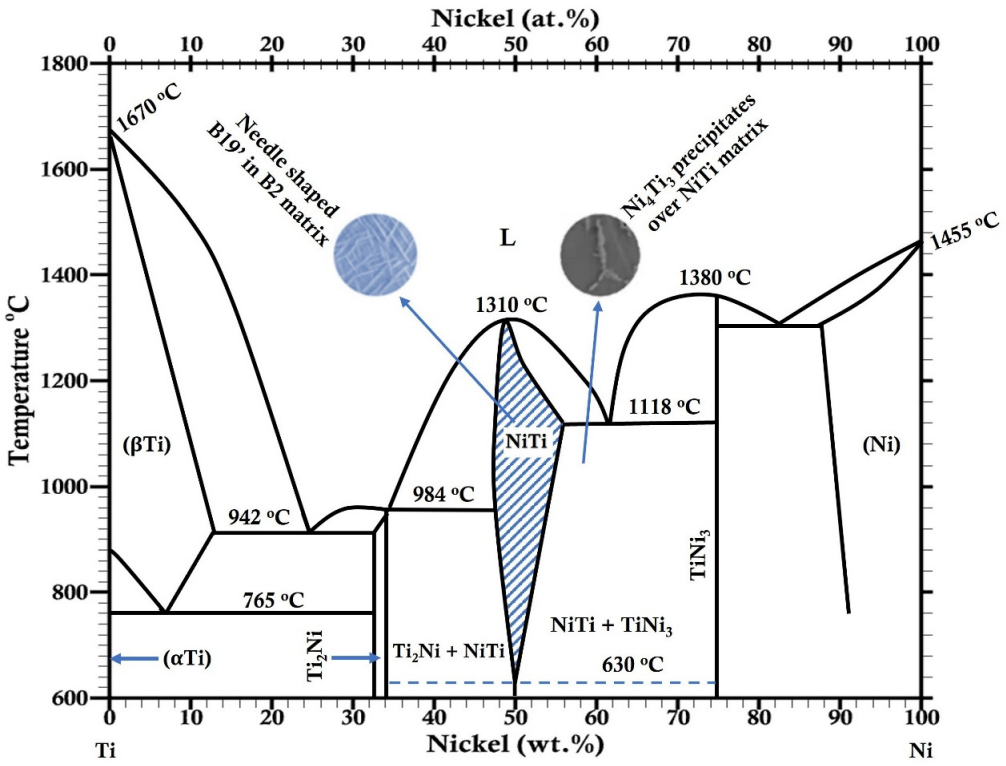

Figure 1. Binary phase equilibrium diagram of NiTi alloy.

Equiatomic NiTi has a higher transformation temperature for SMAs and a higher recoverable strain. On the other hand, NiTi with Ni 50–55 at. % or 55–60 wt.% has specific properties, like lower density, high hardness, high corrosion resistance, and non-magnetic nature, making it very useful in various industries [51]. 55NiTi (55 wt.% Ni (50 at. % Ni)) with a near equal atomic ratio has shape-memory effect and superelasticity. It is a typical shape-memory alloy and has attracted extensive attention from researchers [69,70]. Nickel-titanium alloy with the composition 60 wt.% Ni and 40 wt.% Ti (i.e., 55 at. % Ni and 45 at. % Ti) is referred to as NiTiNOL60 alloy. NiTiNOL60 alloy is a Ni-rich intermetal-

lic nickel-titanium alloy that contains a broad combination of physical and mechanical properties, such as high hardness, low elastic modulus, resistance to aqueous corrosion, and good biocompatibility [11,66,67]. These unique combinations make this alloy an attractive candidate for medical components such as implants and prostheses, where hard and biocompatible materials with low stiffness are typically employed. NiTi-based shape-memory alloys have been shown to exhibit the shape-memory effect (thermally induced transformation) and superelasticity (mechanically induced transformation), depending on the composition, processing methods, and other factors [69]. However, the production technology for NiTiNOL is crucial considering the great affinity of titanium for carbon and oxygen, as well as the requirement to reduce the creation of non-metallic impurities in the elements' involvement. Aside from minimising the formation of non-metallic inclusions, it is essential to achieve an alloy with a precise, stable chemical composition [68]. As a result, high-quality raw materials, those having 99.99 wt.% Ni and 99.8 wt.% Ti, are required for the fabrication of NiTiNOL. According to Stanford [71], the Hot Isostatic Pressing (HIP) method commonly used for the processing and fabrication of 60NiTi alloy is described in NASA's technical report [71,72]. Another study by Khanlari et al. [73] presented Ni-rich 58NiTi and 60NiTi fabricated from elementally blended Ni and Ti powders using a laser powder bed fusion technique.

Nickel and titanium are the two significant elements mostly used in high-temperature applications [19,48]. Superalloys are preferred over conventional materials for such high service temperatures (650 °C), particularly where the structural component may fail due to creep and/or fatigue [31,74,75]. NiTiNOL60 has superior oxidation and corrosion resistance with excellent stable mechanical properties at higher service temperatures [51], leading to its wide medical and engineering applications. Notwithstanding, the previous study by Okoani et al. [76] presented that NiTi-based alloys face significant concern in tribological applications, such as automotive; spacecraft [77]; marine [22,23]; food and beverage processing [78–80]; pharmaceutical [81]; biomaterial [82]; actuators [83]; and biomedical sectors such as orthopaedic [84], endodontic [68], and orthodontic [68].

2.1.1. Medical Applications of NiTi Alloys

The advancement in medicine and material engineering has promoted the utilisation of implant materials, including stainless steel, cobalt-chromium alloy, organic polymer, magnesium matrix composite, nickel-titanium shape-memory alloy, and titanium alloy [85,86]. While biomaterials like ceramics (alumina), polymers (UHMWPE), and metals (titanium and cobalt-chromium alloys) show outstanding biocompatibility, they have their drawbacks, including the potential for hazardous substances in the alloying elements [25,54,57,87]. Titanium alloys are among the metallic materials most commonly employed in biomedical applications [60,88]. They are appropriate as implant materials due to their unique combination of corrosive and mechanical qualities [89]. It is well known that, when exposed to bodily fluids such as saliva, phosphate-buffered saline, etc., all titanium alloys have the ability to form a protective coating that can prevent corrosion [90]. Under these circumstances, the protective layer can delay or stop the dissolution of the metallic ions (without involving any mechanical action) [91]. Still, mechanical loading can damage this layer, thereby releasing metallic ions. Figure 2 illustrates the artificial implant in a hip joint depicting tribocorrosion and fretting corrosion due to tribological interfaces around the hip joints [42,89,92]. As a result, CoCr alloys are frequently combined with Ti alloys to considerably reduce micromotions and fretting corrosion [44,89]; however, metallic materials alloyed with chromium release carcinogenic elements, which can cause serious health issues. Although cobalt-chromium alloy possesses good corrosion resistance and tolerates large loads, both metals possess cytotoxicity [93]. The widely used titanium alloy Ti–6Al–4V is an αβ-type alloy that is associated with toxic alloying elements: vanadium (V) and aluminium (Al). That may result in issues related to the development of Alzheimer's disease and inflammatory cell reactions [89,94]. To combat the problem, NiTi shape-memory alloys and magnesium-based alloys were introduced to satisfy more specialised needs, like

non-conventional reconstructive surgery involving hard tissues or organs (NiTi as vascular stents) and bone tissue engineering and regeneration (magnesium-based alloys). Although magnesium matrix composites and alloys have quick biodegradation rates, they have low mechanical qualities and are not corrosion-resistant [42,82,85]. These have promoted the need to develop biomaterials with a lower modulus of elasticity, increased corrosion resistance, and more acceptable biocompatibility [25,95].

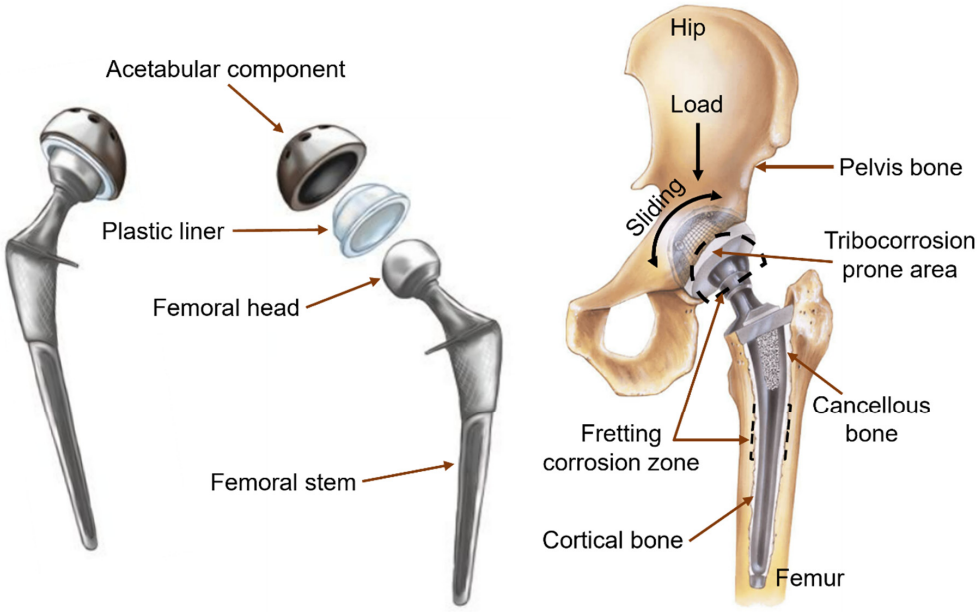

Figure 2. Schematic representation of the tribocorrosion-prone area in a hip joint implant.

Consequently, NiTi alloys are emerging as the optimum choice, as numerous researchers have examined and compared the corrosion and/or tribological properties of these biomaterials to those of other materials, including Ti and its alloys, CoCr alloys, 316L stainless steel, etc. [27,29,96–99]. Buciumeanu et al. [60] investigated the viability of substituting NiTi alloy for Ti-6Al-4V alloy in some medical applications, such as implants. This is because metallic implants designed for medical bone replacement should have characteristics similar to the organic tissue that must be replaced [25,60]. It has excellent biocompatibility; high corrosion resistance; suitable mechanical properties (high strength, sufficient ductility, low Young's modulus, high hardness, etc.); high wear resistance; and osseointegration. Table 1 compares the mechanical properties of cortical bone and some selected metals often used as biomaterials. Given that bone's ultimate compressive strength is less than 340 MPa, implants intended for general bone replacement applications should, as shown in Table 1, have a strength of 340 MPa or above [42,100]. This is because porous structures promote bone in-growth, lower the implant's Young's modulus, and help to lessen the stress-shielding phenomenon. Thus, NiTi-based alloy demonstrates the acceptable characteristics that make it a suitable biomaterial for bone replacement and implant.

Table 1. Comparing the mechanical properties of common implant biomaterials and cortical bone.

Material	Young's Modulus (GPa)	Ultimate Tensile Strength (MPa)	Fracture Toughness (MPa)
Cortical bone	10–30	130–150	2–12
Trabecular bone	0.01–3	2–70	–
NiTi alloy	30–50	1355	30–60
Mg alloy	40–50	100–250	15–40
Ti alloy	105–125	900	~80
316L stainless steel	200	540–1000	~100
CoCrMo alloy	240	900–1540	~100

In orthodontics, following the intricate tribo-electrochemical process in the oral environment, Kassab and Gomes [101] examined the fracture of NiTi wires in artificial oral environments. It is established that there is a considerable risk of corrosion-induced fracture when using super-elastically strained NiTi implants in fluoride-containing oral environments [101,102]. Figure 3 depicts a dental implant using a biomaterial, and in the complex oral environment, ingesting food particles and fluid substances in the presence of saliva results in temperature and pH variations that promote corrosion (fretting) activities. Further actions from chewing food products trigger the micromovements between the implant abutment, the gum tissues, and the jawbone, contributing to the enamel/crown wear and distorting the periodontal ligament. The combined wear and corrosion interactions lead to the tribocorrosion phenomenon.

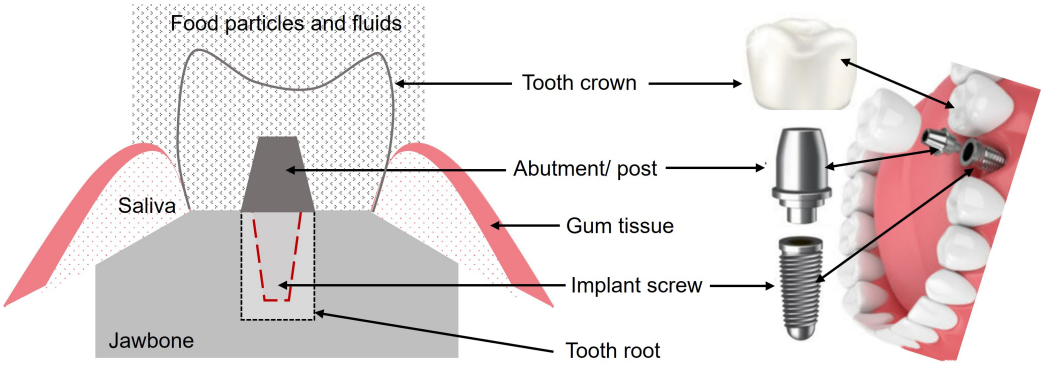

Figure 3. Schematic representation of the tribo-corrosion-affected area in an oral environment.

The invention of NiTi instruments has since proven beneficial to endodontic treatment [103] because of the easier and more effective root canal preparation made possible by their higher taper. Tools manufactured from NiTi alloys have advantages over those made from stainless steel alloys in terms of mechanical qualities, including increased fatigue resistance, high flexibility, and resistance to fracture from twisting in either a clockwise or anticlockwise direction [32,104]. Brantley et al. [89] stated that stainless steel, cobalt chromium, nickel-titanium, and beta-titanium are the four main orthodontic alloys that are currently widely used for orthodontic wires, brackets, and devices. Despite the benefits, each alloy has some associated drawbacks regarding clinical application [89,105,106]. Table 2 summarises the general compositions and mechanical properties of these alloys.

Table 2. Mechanical properties of four major orthodontic alloys [89].

Alloy	General Composition	Elastic Modulus (GPa)	0.1% Yield Strength (MPa)
Stainless steel	Fe–Cr–Ni	160–180	960–1500
Cobalt–chromium	Co–Cr–Fe–Ni	150–180	830–1200
Nickel–titanium	Ni–Ti	32–36	200–550
Beta–titanium	Ti–Mo–Sn–Zr	60–68	620–690

2.1.2. Engineering Applications of NiTi Alloys

NiTi alloys have gained vast engineering applications due to their outstanding corrosion resistance and good mechanical qualities [76]. Ni-based superalloys are used in the aerospace industry for nuclear power plant boilers, turbine blades, and aeroengine casings [51]. Variable geometry chevrons, variable camber fan blades, actuators, bearings, general flow control, adaptive intake nozzles, flaps, and other hinged components are just a few of the aerospace applications for NiTi alloys [69,107,108]. Although they are less common, alloys with higher nickel contents (e.g., 52 to 57 at. % Ni) have several beneficial properties for structural applications, including high hardness, resistance to corrosion, and low density, thereby making these alloys beneficial in tribological and tool manufacturing [109]. Accordingly, Buehler and Wang [67] suggested using these alloys in

non-magnetic hand tools, hardened penetrators, and bearings for water-flooded rotating components. The exceptionally high hardness and low effective modulus ensure this alloy can withstand extreme strains without permanently deforming, which lowers the possibility of structural damage at contact areas during shock loading. Because of these qualities and its superior corrosion resistance, NASA considered using this alloy in the International Space Station's water recycling system in place of bearings [107,110,111].

DellaCorte [112] studied the mechanical components representing severe bearing or gear applications that have long challenged the bearing community. The field of applications was categorised into low, moderate, and critical needs. The study highlighted considerations needed in shock/high loads as critical for aircraft landing gears, space gyros, and mining vehicle bearings. Critical considerations are required for corrosion design requirements in aircraft control surface bearings, landing gears, marine machinery, food processing, and water treatment plants. While X-ray tube bearing requires critical consideration in high-temperature and electrical conduction applications, their study revealed that materials used for X-ray tubes should be compatible with solid film lubricant, tolerate radiation and be able to operate in a vacuum (little or no outgassing tendency) [112].

Near-equiatomic and Ti-rich compositions have typically been used for solid-state actuation in appliances, including those found in spacecraft, automobiles, and marine equipment [77,109]. Moreover, unlike Ti alloys, the combined Ni and Ti materials have been shown to possess hardness comparable to tool steels and the ability to be comparably lubricated [67,110].

2.1.3. Protection Mechanisms Against Tribocorrosion

Different measures such as surface modifications and coatings have been employed in the protection of metallic components against surface deterioration, which is often aggravated by tribocorrosion [3,113–115]. The benefit of this protective layer is to promote longevity of the components and decrease the manufacturing cost [116]. According to Fotovvati et al. [114], the different coating methods, materials, and applications all tend to a common purpose of protecting a part or exposed structure to mechanical or chemical damage (i.e., tribocorrosion). Dong et al. [117] investigated the erosion wear behaviour of NiTi alloy coating fabricated via high-frequency induction heating technology. Shen et al. [118] studied the enhanced anti-tribocorrosion performance of Ti-DLC coatings deposited on steel substrate using a filtered cathodic vacuum arc (FCVA). According to their report, the Ti-DLC coatings at −200 V presented the best anti-tribocorrosion performance with the least values of friction coefficient and wear rates, thereby suggesting that Ti-DLC coating is a potential protective material for marine equipment. In another study, López-Ortega et al. [119] investigated the performance of a thermally sprayed aluminium (TSA) coating modified by the plasma electrolytic oxidation (PEO) technique for offshore submerged components protection. The results showed that the TSA coating modified by PEO showed a significant improvement in the corrosion, wear, and tribocorrosion resistance, leading to smaller material losses and lower coefficient of friction (COF) [119]. Dong et al. [91] presented the surface-modified techniques and emerging functional coating of dental implants. They attributed the major reasons for implant failure to poor osseointegration and bacterial infection. Some researchers have investigated the effects of graphene on tribocorrosion behaviour [39,40]. For improved surface protection, further research into the development of more advanced coating techniques is required.

2.2. Tribology and Tribological Concepts

Figure 4 presents a summarised representation of tribological concepts during reciprocating sliding. As is known, tribology encompasses the wear, friction, and lubrication of a material, while friction is an underlying force that impacts almost all interface-related applications. The interface-related applications could be categorised from solid–solid and solid–liquid to liquid–liquid interfaces [120]. Friction is often associated with mechanical wear; hence, controlling its level between the contact surfaces of two moving bodies is

necessary. The coefficient of friction is used to measure friction, and it can be calculated using Equation (1) as follows:

$$\mu = \frac{F_t}{F_n} \tag{1}$$

where μ = the coefficient of friction, F_t = tangential force, and F_n is the normal load applied on the moving body.

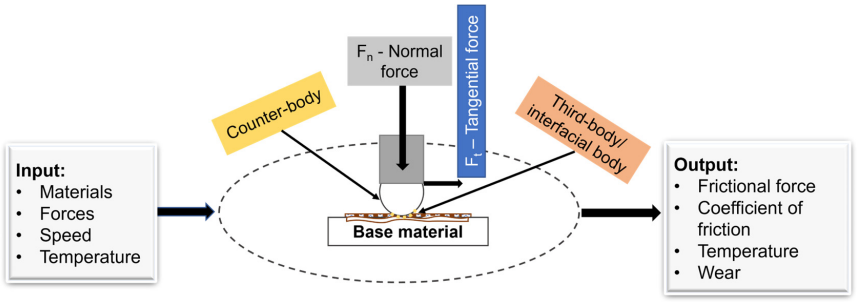

Figure 4. Schematic representation of a tribological system.

Leonardo da Vinci first introduced the fundamental understanding of interfacial friction through the distinction between motion resistance in sliding and rolling motions, as reported by Yi et al. [120]. Recent investigations on macroscopic interaction have evaluated the impact of load, contact area, and sliding speed on macroscopic solid motions. Figure 5 depicts the combined effect of load and sliding speed on the sliding wear process in metals [121]. The image shows increased temperature at the contact interface, heavy mechanical damage at higher loads, and increased sliding speed, resulting in plastic deformation and wear loss.

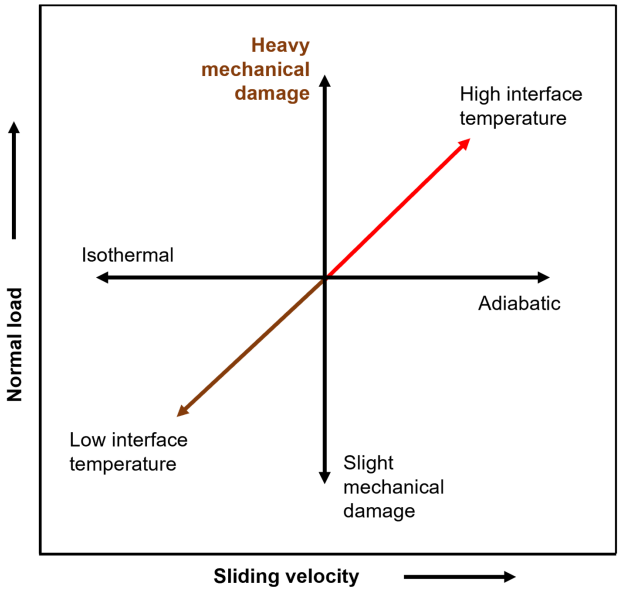

Figure 5. Effect of load and sliding speed on the sliding wear process in materials.

Since wear occurs due to relative motion between two surfaces, surface damage during wear is mainly related to the surface of the two contact materials and environmental conditions under lubricated and/or unlubricated systems. Several wear equations in the literature can be used to quantify wear and theoretically determine the amount of material loss. This includes Archard's law, a simple equation (Equation (2)) used in wear analysis to compute material loss (wear volume).

$$\frac{V}{L} = K\frac{F_n}{H} \tag{2}$$

where V = wear volume loss (mm^3), L = total sliding distance (m), F_n = applied normal load (N), H = hardness of the material (MPa), and K = wear coefficient (non-dimensional).

However, there are some drawbacks, because the equation does not consider the effect of sliding speed, contact area, interface temperature, lubrication, etc. Measuring the wear rate of a material in the absence of corrosion is required to determine the pure mechanical wear. This can be accomplished with a sliding wear test that solely utilises tribological factors. Profilometry is a technique for quantifying material loss through experimentation. By measuring the height and width of profiles across the wear track, this technique aids in identifying materials removed or displaced in sliding contact.

Sliding Wear Mechanisms of NiTi-Based Alloys

Different wear mechanisms can be identified depending on the relationship between the interactions between a material's mechanical properties, applied load, and contact pressure. Wear can generally be classified into adhesive wear (this occurs based on the micro-joints between the two surfaces during relative motion), surface fatigue wear (occurs during cyclic loading), corrosion wear (usually accelerated by oxidation in a corrosive environment), and abrasive wear (occurs as ploughing or cracking when a hard surface slides against a softer surface) [8,122]. Since the elastic or reversible deformation occurs when the average contact pressure is lower than the yield strength of the contacting material, repeated rolling/sliding results in crack initiation and propagation, leading to fatigue wear. Plastic or irreversible deformation occurs when the average contact pressure exceeds the yield strength of a material. A different wear mechanism known as cutting or micro-cutting happens when the high strain created at the indenter edges causes the sharp edges of sliding bodies to cut through areas of the softer sliding material. When there are blunt asperities, the moving indenter uses a process known as ploughing to drive the materials in the contact zone apart [8,121,122]. The wear rate estimations can quantify the material loss or removal per unit time. As represented in Figure 6, Hutchings [121] described the relationship between wear rate and contact resistance on a logarithmic scale, i.e., the wear behaviour of a material sliding against a smooth, hard surface, as a function of the normal load [121].

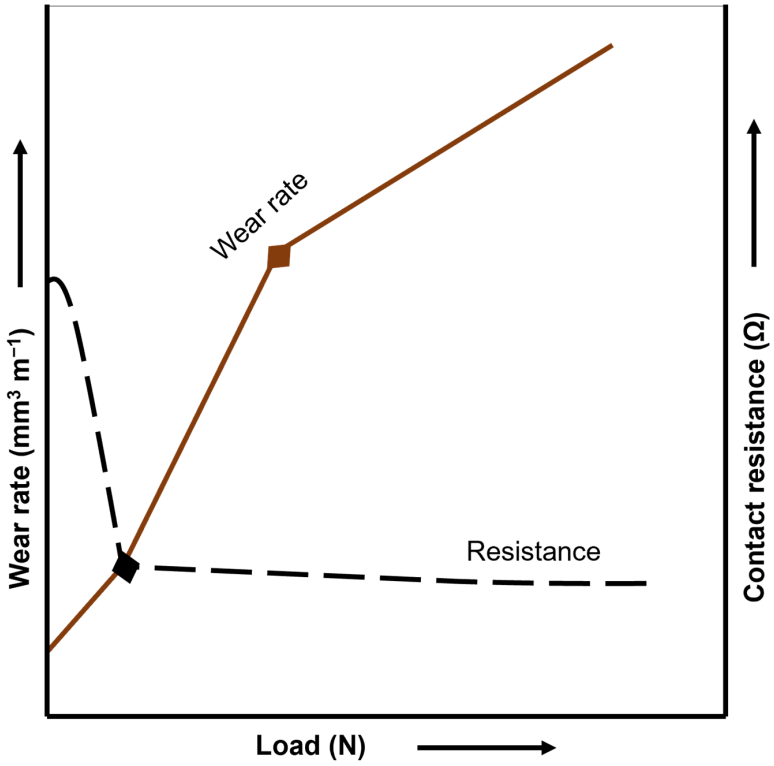

Figure 6. The relationship between wear rate and electrochemical contact resistance.

As depicted in Figure 6, it is evident that Archard's equation (Equation (2)) is obeyed, whereby, at higher loads (depending on the contact geometry) leading to significantly higher contact pressures, the wear rate increases significantly. Higher contact resistance is often recorded at low loads, because the local contact pressure at asperities contacts is inadequate to penetrate the passive oxide film. Hence, insufficient contact pressure significantly increases the wear rate by approximately 100. This wear transition is attributed to the presence of a thin oxide film at the contact surfaces [8].

2.3. The Fundamentals of Corrosion

Corrosion is the reaction (chemical, electrochemical, physical, or combination) of a material and its environment with a consequent deterioration in its properties. While the corrosion phenomenon is related to the material, the environment, and the interface between both, this study focuses on the electrochemical reaction of materials under tribological contacts. The interaction of a metal and a corrosive environment reveals that the oxidising agent oxidises metal. Various electrochemical interactions show that factors influencing corrosion include the position of the metal in the electrochemical series, pH, electrolyte concentration, impurities in the metal, concentration of oxygen, and temperature difference [31,123]. Two common surface reactions in aqueous electrolytes or a specific corrosive environment are the cathodic (oxidising agent-induced electron consumption) and anodic (metal atom electron removal) reactions [6,20]. The following chemical reactions represent the anodic and cathodic half-cell reactions during the electrochemical process (Equations (3)–(5)).

$$M \rightarrow M^{+z} + ze^{-} (\text{Oxidation} \equiv \text{Anodic}) \quad (3)$$

$$zH^{+} + ze^{-} \rightarrow H_z \uparrow (\text{Reduction} \equiv \text{Cathodic}) \quad (4)$$

$$M + zH^{+} \rightarrow M^{+z} + H_z \uparrow (\text{Redox} \equiv \text{Overall}) \quad (5)$$

The material undergoes various electrochemical responses through the immune state (where the metal is not corroded), active state (corrosion leading to metal loss or dissolution of one of the constituents of the corrosive environment into the metal), and the passive state (metal generates a protective oxide passive film on its surface, which reduces the corrosion rate). Corrosion damage in the form of general or localised corrosion can be used to determine the corrosion mechanism. Metals with low corrosion potential will undergo anodic polarisation, increasing the anodic dissolution rate. The metal with a high corrosion potential will undergo cathodic polarisation, slowing the dissolution rate down [124]. Pitting, the conventional corrosion form, exists in different stages, even though pitting is self-initiating and self-propagating, making it difficult to determine the borders for every stage, including the nucleation, metastable pit formation, and stable pitting [125].

Corrosive Wear Mechanisms of NiTi-Based Alloys

Most metals and alloys face surface deterioration when in contact with water-based corrosive environments. According to Equation (6), the reaction between metal and water generates a surface metal oxide and releases hydrogen [126,127].

$$Me + H_2O \rightarrow MeO_x + xH_2 \quad (6)$$

As reported by Vilhena et al. [45], the electrochemical behaviours (reduction reactions) that take place at the cathodic branch are dependent on the nature of the corrosive environment and are summarised as follows in Equations (7)–(10):

$$O_2 + 4H^{+} + 4e^{-} \rightarrow 2H_2O \,(\text{Oxygen reduction in acidic medium}) \quad (7)$$

$$O_2 + 2H_2O + 4e^{-} \rightarrow 4OH^{-} \quad (\text{Oxygen reduction in alkaline environment}) \quad (8)$$

$$2H_2O + 2e^{-} \rightarrow 2OH^{-} + H_2 \quad (\text{Water reduction in neutral/alkaline medium}) \quad (9)$$

$$2H^+ + 2e^- \rightarrow H_2 \quad \text{(Proton reduction in an acidic environment)} \tag{10}$$

During the electrochemical activities on metal surfaces, corrosion can be uniform or localised. Other common forms of corrosion include:

- Stress corrosion cracking: Occurs when a metal under stress cracks in a corrosive environment.
- Galvanic corrosion (two-metal corrosion): Occurs when two dissimilar metals in electrical contact are exposed to an electrolyte.
- Pitting: Formed by small anodes on a metal surface, creating holes or pits.
- Intergranular corrosion: Occurs at or near grain boundaries in a metal.
- Crevice corrosion: Localised corrosion that occurs in crevices, shielded areas where stagnant solution can form.
- Erosion corrosion: Occurs due to the combined effects of corrosion and relative motion of a corrosive fluid on a metal surface.
- Selective leaching or dealloying: Preferential removal of one element from a solid alloy by corrosion.

3. Tribocorrosion: Historical Background and Concept

The history of tribocorrosion (tribo-electrochemistry) dates back to 1875 when Edison observed a variation in friction coefficients at various applied potentials [57]. Tribocorrosion can be described as a degradation phenomenon of material surfaces (wear, cracking, corrosion, etc.) subjected to the combined action of mechanical loading (friction, abrasion, erosion, etc.) and corrosion attack caused by the environment (chemical and/or electrochemical interaction), as highlighted in Figure 7.

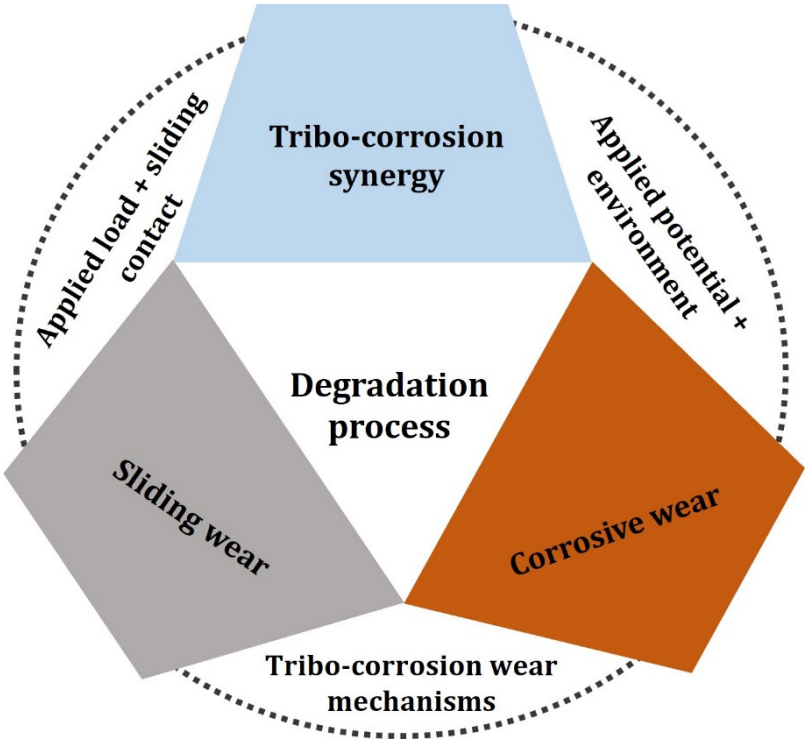

Figure 7. Schematic illustration of the tribocorrosion concept.

Material degradation due to simultaneous chemical and mechanical effects may occur under various conditions and contact modes, as shown in Figure 7. According to Siddaiah et al. [12], tribocorrosion is a surface alteration that involves the joint action of relatively moving mechanical contact with electrochemical reactions [12]. It measures the tribological quantities, such as friction and wear, in a controlled and reproducible manner, as well as the electrochemical interactions of the system. Two-body or three-body contacts

between sliding surfaces are a common cause of tribocorrosion. The relative motion of the surfaces can be unidirectional, as in the case of a pin-on-disk wear test apparatus or reciprocating. Fretting involving a reciprocating motion of small magnitude is a particular type of tribological contact. Rolling contact occurring in ball bearings also experiences tribocorrosion. Particle impingement happens in erosion corrosion as a combination of mechanical and chemical attacks on materials in pumps and pipes carrying slurries. The distinctive features of the tribocorrosion mechanism, tribology, and corrosion actions are influenced by environmental factors [6], as presented in Figure 8.

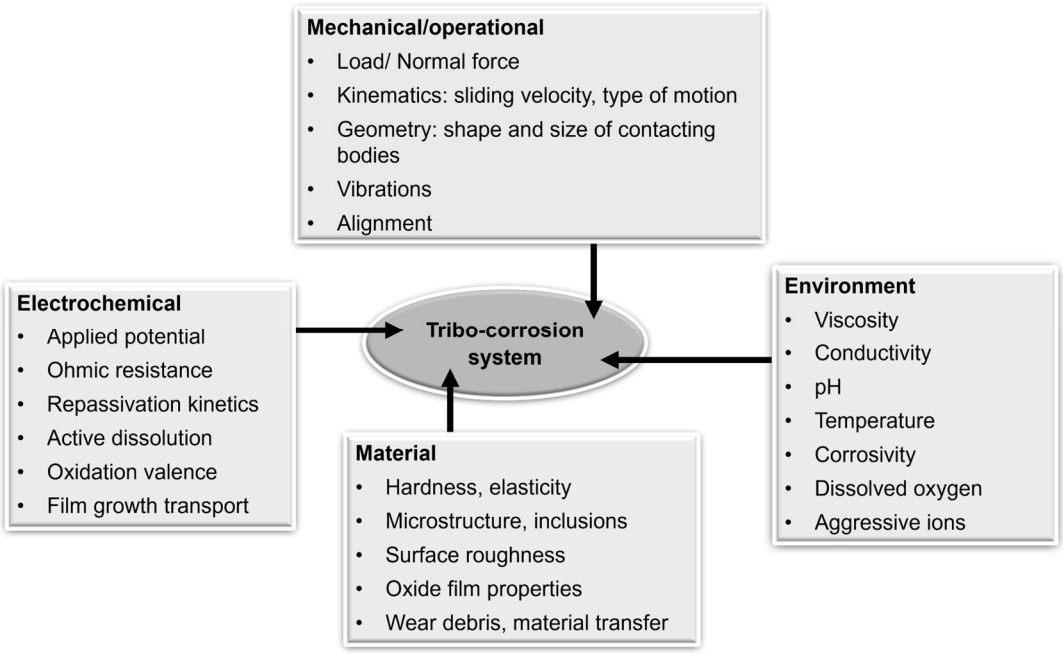

Figure 8. Factors influencing tribocorrosion.

Considering the impact of the relative motion in erosion-corrosion issues, Wellman [128] highlighted the relationship between sliding velocity and temperature in Table 3.

Table 3. Examples of industrial erosion corrosion issues as a function of the sliding velocity and temperature [128].

	Low Temperature	High Temperature
Low velocity	Offshore and marine structures Slurry transportation of solids Chemical processing Exhaust valves	Fluidised bed Combustors Coal-fired boilers Chemical processing Aero engines
High velocity	Oil and gas industry Mining Fuel injection systems	Oil and gas industry Steam turbines Gas turbines Turbochargers

3.1. Tribo-Electrochemical Test Procedures for Sliding Contacts

To investigate the tribocorrosion behaviour of a material, mechanical and corrosion responses must be collected and monitored during tribocorrosion testing [129–134]. Figure 9 shows the schematic representation of a tribocorrosion system.

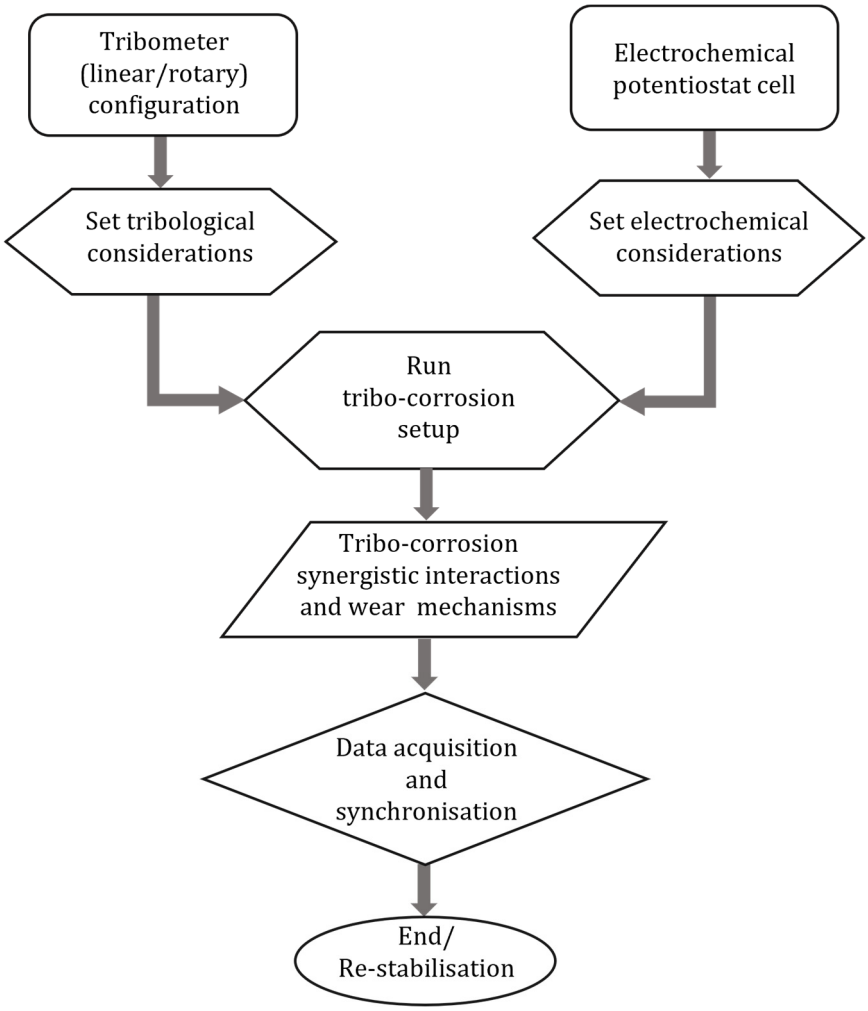

Figure 9. Schematic flowchart for tribo-corrosion experimental setup.

As shown in Figure 9, the tribometer measures the evolution of frictional forces and other tribological properties as it creates relative motion in either unidirectional (rotatory) or bidirectional (reciprocating) sliding of two surfaces against each other. On the other hand, an electrochemical technique/potentiostat cell is employed to monitor the corrosion response from the test system [57,132]. Hence, typical electrochemical interfacing consists of three electrode configurations, including (1) a reference electrode (RE) (saturated calomel electrodes (SCE) or silver/silver chloride electrodes (Ag/AgCl)) with a stable, well-defined potential, (2) a counter electrode (CE) made of inert material (graphite rod or platinum wire), and (3) a working electrode (WE) often the specimen under investigation. The electrode configurations are coupled to a potentiostat to register the potential between the reference electrode and the working electrode or the current between the counter electrode and the working electrode. Okoani et al. [76] presented a schematic representation of a typical tribocorrosion test setup for a linear reciprocating ball-on-plate configuration in their study.

3.2. Tribocorrosion Wear Mechanisms

Numerous studies have examined the tribocorrosion behaviour of NiTi alloy in various corrosive media and test conditions [5,84,135]. These studies report that the degradation caused by the combined effects of mechanical and electrochemical processes is generally distinct from these failure mechanisms operating independently [60]. For example, a 2014 study by Kosec et al. showed that, while artificial saliva increased the wear of NiTi, mechanical loading caused corrosion to accelerate [21,136]. At the onset of sliding during

the tribocorrosion process, titanium alloys and other passive metals undergo a sudden drop in the initial corrosion resistance, E_{oc} [132,137]. This is explained by destroying a thin passive layer along the wear track and exposing the electrolyte to new metal surfaces [123]. Passive metals are particularly susceptible to tribocorrosion, because sliding can easily remove the passive film's protective properties, causing a rapid corrosion rate before the surface repassivates [96,132,138]. The metal in the worn track experiences the following oxidation processes, which result in the formation of soluble ions and/or solid corrosion products [129,139]:

$$M \rightarrow M^{n+} + ne^{-} \quad (11)$$

$$M + n/2H_2O \rightarrow MO_{n/2} + nH^{+} + ne^{-} \quad (12)$$

To account for wear after the electrochemical measurements, the wear track is considered to consist of two distinct zones: the active area, A_{act}, where the initial passive film has been removed, and the passive area, A_{repass}, where the film was either not removed or it had enough time to be restored. The surface area of the wear track, A_{tr}, is considered the surface area measured at the end of the sliding test, with $A_{tr} = A_{act} + A_{repass}$. The material loss in the wear track, W_{tr}, is decomposed into components connected to the different wear track zones in the wear track, as mathematically shown by Azzi and Klemberg-Sapieha [129]:

$$W_{tr} = W^{c}_{act} + W^{m}_{act} + W^{c}_{repass} + W^{m}_{repass} \quad (13)$$

where W_{tr} = material loss along the wear track, W^{c}_{act} = material loss due to corrosion of active material, W^{m}_{act} = material loss due to mechanical wear of active material, W^{c}_{repass} = material loss due to corrosion of repassivated material, and W^{m}_{repass} = material loss due to mechanical wear of the repassivated material.

Further, the mechanistic interpretation [140] of the tribocorrosion phenomenon [7] i.e., the total wear volume (V_t) as the sum of the material loss due to sliding wear (V_{mech}) and the loss of material due to corrosion or electrochemical oxidation (V_{chem}), is shown in Equation (14) [141]:

$$V_t = V_{mech} + V_{Chem} \quad (14)$$

Using the wear volume, the specific wear rate can be estimated from Archard's wear law, Equation (2).

$$\text{Specific wear rate} = \frac{\text{wear volume}}{\text{normal load} \times \text{sliding distance}} \quad (15)$$

From a physical point of view, tribocorrosion includes a variety of mechanical and chemical degradation phenomena, namely, corrosive wear, erosive wear, wear-accelerated corrosion, erosion corrosion, oxidative wear, fretting corrosion, stress corrosion cracking, and corrosion fatigue. The simultaneous wear and corrosion actions lead to an irreversible transformation of the material occurring at a tribological contact [142]. The continual sliding between the interacting bodies results in wear, i.e., particle detachment and particles trapped at the interfaces, which are referred to as third bodies, as shown in Figure 10. These third body particles can oxidise and/or spread to cover one or both surfaces (forming a transfer film). The film or accumulation of third bodies alters the contact conditions of the initial bodies, and the resulting wear can be explained as a mass flow between the interacting bodies and the third bodies [8]. The mechanical abrasion of passive film usually leads to wear-accelerated corrosion due to the high chemical reactivity of the bare metal surface exposed to the corrosive environment. On the other hand, the passive films seem to decisively influence the surface mechanical response of metals and the third body behaviour. Under tribocorrosion conditions, two main mechanisms contribute to material removal from the surface: wear-accelerated corrosion and mechanical removal from the sliding contact [20,132,139].

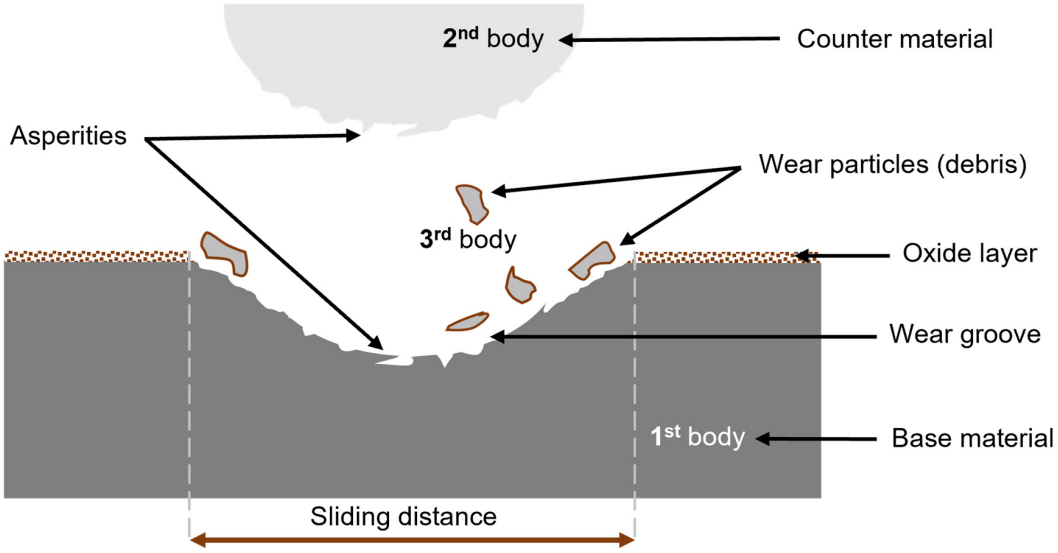

Figure 10. Representation of a third body wear phenomenon during tribocorrosion.

3.3. Tribocorrosion: Current Status, Challenges, and Prospects

3.3.1. Current Status and Challenges

Fundamentally, tribocorrosion studies deal with an irreversible transformation of materials or their function due to simultaneous mechanical and chemical/electrochemical interactions between surfaces in relative motion [4,143]. As stated earlier, tribocorrosion is a complex phenomenon due to simultaneous actions that adversely affect each other. Recently, research in tribocorrosion has received significant attention, because the process occurs in almost all engineering and some medical applications. Thus, tribocorrosion has become a subject of intense study, attracting researchers from different fields based on the multidisciplinary approach of the systems involved. Table 4 presents a summarised update on the recent tribocorrosion reviews. Notably, research on tribocorrosion in medical applications has up-to-date information compared to engineering applications, where the last review was in 2018.

Table 4. Summary of review papers on tribocorrosion and NiTi in the past decade.

Title and Reference	Remark/Recommendation
A review on wear, corrosion, and wear-corrosion synergy of high entropy alloys [144].	Their study comprehensively evaluated the critical developments in wear, corrosion, and wear–corrosion resistance made by high entropy alloys (HEAs) over the previous 20 years. According to their study, scientists interested in studying the tribocorrosion of recently designed and manufactured HEAs have several difficulties due to the need for more pertinent papers on wear–corrosion synergy. Thus, the conclusion is that this relatively uncharted area awaits exploration by more researchers to understand the wear–corrosion synergy of HEAs fully.
Recent approaches to limit the tribocorrosion of biomaterials: A review [44].	Their analysis of the literature gave an overview of the research trend. The ability to create lifelong biomaterial apparatuses should be a key component of biomaterials research and development. Accordingly, a new wave of research was first essential to understand the intricacy of biomaterials' interactions with the human body and then attempt to produce the necessary devices to fulfil our needs.
(Bio)Tribocorrosion in dental implants: Principles and techniques of investigation [4].	In the domains of tribology and medicine, the highlighted problems in the review, such as the prevention or minimisation of tribocorrosion in biological tribopairs, etc., undoubtedly represent a scientific challenge for the upcoming years.
Nickel-titanium alloys as orthodontic archwires: A narrative review [145].	The study evaluated NiTi archwires from a clinical perspective, focusing on mechanical properties and the effects of tooth alignment, biofilm formation, and Ni ion release. The authors anticipate that their findings will shape the future of the NiTi archwire field in terms of welding different types of archwires, computational methods, and improvement in coating technologies.

Table 4. *Cont.*

Title and Reference	Remark/Recommendation
New thermomechanically treated NiTi alloys–A review [97].	The study examined various exclusive methods of manufacturing nickel-titanium (NiTi) alloy to enhance the mechanical characteristics of NiTi endodontic devices. As previously mentioned, thermomechanical treatment of NiTi alloy permits a shift in phase composition that, in clinical settings, manifests as martensite or R-phase. Compared to ordinary NiTi, thermomechanically treated NiTi alloys claim to have a larger deflection angle at failure and to be more flexible, with improved cyclic fatigue resistance.
60NiTi: A review of recent research findings, potential for structural and mechanical applications, and areas of continued investigations [146].	This article summarises and evaluates a wide range of previous and current research on 60NiTi to identify areas that need more investigation. Specifically, recent findings show that wear and friction behaviour are inherently contradictory. Their work indicated that more research is necessary to fully understand how alloying affects other characteristics, mainly wear. It is anticipated that, as the knowledge and development of this alloy improve, its use in various applications will rise.
Tribocorrosion of passive materials: A review on test procedures and standards [132].	They reviewed the test protocols and electrochemical methods used to evaluate the tribocorrosion behaviour of passive materials over the last few decades. As mentioned in their study, a test protocol suggested by several authors to remedy the drawbacks of the ASTMG119 standard served as the foundation for developing the UNE 112086 standard (UNE 112086: 2016). They also shed light on the electrochemical methods and investigations made by tribocorrosion researchers.
Significance of tribocorrosion in biomedical applications: Overview and current status [57].	They focused on orthopaedic surgery and dentistry to highlight the complexity of tribocorrosion processes and provided an overview of bio-tribocorrosion.

A detailed study of the tribocorrosion mechanisms was recently initiated in different fields to clarify the extent of interacting material surfaces. As a result, many researchers have investigated several studies on tribocorrosion to explore the underlying mechanisms of this interlinked phenomenon. A significant area of focus is understanding the synergistic interactions of the testing parameters of the system. Therefore, this results in the need to develop a mechanistic model considering the interlinked actions of sliding wear, electrochemical corrosion, passivation and repassivation, and other surface/morphological impacts. A clear understanding of the tribocorrosion synergistic interactions and mechanisms would allow accurate predictions to quantify the effects of various operating parameters through theoretical and/or empirical models. Therefore, much more research must be required to reveal the drawbacks of tribocorrosion of 60NiTi alloy and its metallurgical relatives. Accordingly, researchers have investigated several studies on the tribocorrosion of NiTi alloys and other similar materials. Table 5 summarises the tribocorrosion studies conducted so far, but it is evident that the researchers mainly focused on biomedicals, lubrication, and sliding wear [26,60,147,148], with little insight into the underlying mechanisms of wear–corrosion synergy.

The current status of tribocorrosion in some selected applications of NiTi-based alloys is outlined as follows. It is established that NiTi alloys have gained attention in marine and offshore applications following the report of López-Ortega et al. [149]. Lopez et al. stated that tribocorrosion is a crucial failure cause in offshore applications due to the synergistic effects of wear and the corrosiveness of seawater. In their work, they investigated the effect of temperature on the tribocorrosion behaviour of two steel grades [31]. Considering the aforementioned extreme conditions, another study conducted by Guadalupe et al. [126] investigated tribocorrosion in pressurised water reactors (PWRs) in harsh environmental conditions (elevated temperature and high pressure). Their study focused on modelling tribocorrosion in PWR based on a mechanistic appraisal of mechanical and chemical loading [126]. To gain a better knowledge of the tribocorrosion performance of NiTi alloy in marine environments, Yan et al. [141] examined the microstructure, phase, and tribocorrosion behaviour of 60NiTi alloy in a simulated seawater environment. According to their research, material loss under tribocorrosion circumstances is significantly influenced

by the synergistic impact between wear and corrosion [141]. Moreover, the following order shows a decrease in the contribution to the overall material loss: corrosion-induced wear (ΔW_c) > pure wear (W_0) > wear-induced corrosion (ΔC_w) > pure corrosion (C_0). The corrosion and wear interplay in the tribo-electrochemical behaviour of the NiTiNOL60 alloy in sulfuric acid and alkaline media were examined in our previous study [76,150]. The findings demonstrated that oxidative wear dominates in the electrochemical regime and causes a cathodic shift during potentiodynamic polarisation measurements, while abrasive wear is the primary mechanism under reciprocating sliding [76,151]. In a different study, Kosec et al. [21] examined the effects of various surface finishes and the microstructures of superelastic NiTi sheets and orthodontic archwires while examining their electrochemical and tribocorrosion capabilities. The results of their investigation demonstrated that the measured electrochemical and tribocorrosion parameters were significantly influenced by the microstructure of the alloys under investigation [21,53,136].

Table 5. Summary of selected works showcasing the tribocorrosion investigations, employed test parameters, and the findings over the past 15 years.

Title and Reference(s)	Tribometer Configuration	Counter Body	Applied Load and Temperature	Scan Rate and Sliding Speed	Electrolyte and Electrode	Findings
Comparative study of the tribocorrosion performance of nitinol60 in acidic, alkaline, and saline environments [5].	Bidirectional ball-on-flat configuration	Ø 10 mm Al_2O_3 ball	3, 5, and 8 N Room temp. (RT) 22 °C	2 mV/s 4 Hz	H_2SO_4, NaOH, 3.5% NaCl. Calomel, Graphite rod	The study revealed that the pH of the corrosive environments played a significant role in the tribocorrosion process). The highest wear volume was recorded in the saline medium. Shear forces caused grain deformations in the alkaline solution. While in an acidic medium, the electro-mechanically induced transformations promoted various wear patterns.
Microstructure, phase and tribocorrosion behavior of 60NiTi alloy [141].	Unidirectional rotating (ball-on-disc)	Ø 5 mm Si_3N_4 ball	1, 5, and 10 N RT	2 mV/s	Artificial seawater. Calomel, Platinum	They employed a systematic tribocorrosion test to study the tribocorrosion performance of 60NiTi alloy thoroughly. Their findings show that the negative synergy between electrochemistry and tribology increases material loss.
The tribocorrosion behaviour of NiTi alloy [21].	Reciprocal/reciprocating (pin-on-disc)	Ø 6 mm Al_2O_3 ball	1 to 5 N RT	0.1 mV/s, 1 mV/s 5 mm/s	Artificial simulated saliva. Ag/AgCl, Platinum	The superelastic NiTi sheet and orthodontic archwire were studied considering their microstructures and the effect of different surface finishes. The study confirmed that the investigated alloys' microstructure significantly affected the measured electrochemical and tribocorrosion properties.
Corrosion and wear interplay: Tribo-electrochemical evaluation of NiTiNOL60 alloy in sulfuric acid [76].	Reciprocating ball-on-flat configuration	Ø 10 mm Al_2O_3 ball	3, 5, and 8 N RT	2 mV/s 4 Hz	Sulfuric acid. Calomel, Graphite rod	Their findings demonstrated that tribo-chemical wear influences several wear mechanisms, with delamination and microcracks notably prominent under higher applied loads.
Tribocorrosion behaviour of NiTiNOL60 alloy in an alkaline environment [150].	Reciprocating ball-on-plate configuration	Ø 10 mm Al_2O_3 ball	3, 5, and 8 N RT	2 mV/s 4 Hz	Alkaline solution Calomel, Graphite rod	The investigation shows that sliding action and wear mechanisms on the tribological wear track have distorted the microstructure grains, leading to the elongation of grains in the direction of sliding wear.
Tribo-electrochemical investigation of 60NiTi alloy in saline solution [152].	Linear reciprocating ball-on-flat configuration	Ø 10 mm Al_2O_3 ball	3, 5, and 8 N RT	2 mV/s 4 Hz	Saline solution Calomel (SCE), Graphite rod	The study highlighted the impact of mechanical forces and electrochemical activities on the surface of 60NiTi alloy. The continuous reciprocating sliding subjected the contact surfaces to fatigue wear, leading to surface deterioration and plastic deformation.
Tribocorrosion behavior of NiTi alloy as orthopedic implants in Ringer's simulated body fluid [84].	Ball-on-disk rotary wear tester	Ø 25.4 mm ZrO_2 ball	0.2, 0.5, 1.0, and 2.0 N RT	7.5 mV/s 75 rpm	Ringer's simulated body fluid. Saturated calomel electrode (SCE), Platinum sheet	Particle concentration and applied load effects were taken into account. The wear component of the material loss was more significant than the corrosion component, indicating wear accountability for the material loss. The primary wear mechanism is two-body abrasive wear, with mechanical abrasion predominating in the corrosion–wear regime.
Tribocorrosion behavior of NiTi biomedical alloy processed by an additive manufacturing laser beam directed energy deposition technique [60].	Reciprocating ball-on-plate configuration	Ø 10 mm Al_2O_3 ball	1 N 37 ± 2 °C	1 Hz	Phosphate buffered saline (PBS) solution SCE	The study demonstrated how additive manufacturing techniques, like LB-DED, can enhance NiTi alloy's wear and corrosion resistance. The improvement in LB-DED NiTi alloy's wear and corrosion behaviour in the presence of PBS solution suggests it is less susceptible to releasing metallic ions than the conventional Ti-6Al-4V alloy.
Tribocorrosive study of new and in vivo exposed nickel titanium and stainless steel orthodontic archwires [96].	Reciprocal tribometer	Ø 6 mm Al_2O_3 ball	37 °C and RT	0.33 mm/s	Simulated saliva Ag/AgCl, Platinum	The comparison revealed that the in vivo exposed archwires had a higher rate of mechanical wear and more corrosion wear. Compared to the new archwires in simulated saliva, the in vivo exposed NiTi and SS archwires showed better electrochemical properties.

Table 5. *Cont.*

Title and Reference(s)	Tribometer Configuration	Counter Body	Applied Load and Temperature	Scan Rate and Sliding Speed	Electrolyte and Electrode	Findings
Microstructure and tribocorrosion properties of NiTi/AlNi2Ti ternary intermetallic alloy [153].	Ball-on-flat reciprocating sliding tribometer	Ø 6 mm Al_2O_3 ball	5 N RT	2 mV/s 1 Hz	0.5 mol/L H_2SO_4 (SCE), Platinum sheet	The study created a novel corrosion-resistant NiTi/AlNi2Ti alloy using an arc melting process. According to the tribocorrosion results, the OCP of the NiTi/AlNi2Ti alloy decreases as sliding begins and then gradually increases during passivation. The OCP value decreases in direct proportion to the increase in frictional force, suggesting a strong wear–corrosion synergistic effect.
Analysis of microstructure, mechanical properties, wear characteristics and corrosion behavior of SLM-NiTi under different process parameters [154].	MFT-5000 multifunctional friction and wear testing machine	4 mm stainless steel quenched steel ball	10 N 37 ± 0.5 °C and 25 ± 0.5 °C (RT)	5 mm/s	SBF and 3.5 wt.% NaCl SCE, Ag/AgCl, Platinum	They investigated the effects of process variables (high P, high V and low P, low V). The results indicate that low P and low V are more favourable to creating the B19′ martensite phase, while high P and high V favour the formation of the B2 austenite phase. The samples have roughly the same coefficient of friction (0.6), but the LP sample is more resistant to corrosion, while the HP sample has superior stability and resistance to friction.
Tribological and tribocorrosion behavior of nickel sliding against oxide ceramics [155].	Linear reciprocal tribometer	Ø 6 mm alumina and zirconia balls	2.74 N	2 mV/s 1 Hz, 20 mm/s	0.1M citrate buffer sol. Mercury sulphate electrode (MSE), Platinum wire	They discovered a linear correlation between nickel and alumina wear. Under passive conditions (no oxide film), alumina and zirconia were found to be worn, but not under cathodic conditions. Nickel rubbing against an alumina ball containing nickel, aluminium, and oxygen forms a tribolayer during sliding in dry conditions.
Tribocorrosion behaviors of Ti-6Al-4V and Monel K500 alloys sliding against 316 stainless steel in artificial seawater [138].	Ring-on-block test rig	49.22 mm × 13.06 mm was made of 316 stainless steel	100 N RT, 25 ± 1 °C	10 mV/s 0.5 m/s	Artificial seawater and distilled water SCE, Platinum plate	In both distilled water and seawater, 316 stainless steel suffers more severe wear when sliding against Monel K500 alloy, more than when sliding against Ti-6Al-4V alloy. However, the wear loss of 316 stainless steel is greater in distilled water than in seawater when sliding against Ti-6Al-4V alloy, which could result from the protective effect of galvanic corrosion.
Mechanical and chemical mechanisms in the tribocorrosion of a Stellite type alloy [156].	Reciprocating (ball-on-plate)	Ø 6 mm Al_2O_3 ball	1.1, 5.8, 11.7, and 17.5 N	2 mV/s 1 Hz, 20 mm/s	0.5 H_2SO_4 solution Mercury sulphate, Platinum coil	The findings indicate that the tribocorrosion behaviour of this alloy is significantly influenced by the current electrochemical circumstances (presence or absence of a passive film). Considering the influence of the passive film, Archard's wear law and existing models for wear-accelerated corrosion could adequately characterise the effect of electrode potential and normal load on the overall degradation by tribocorrosion.
Influence of temperature on the corrosion and tribocorrosion behaviour of high-strength low-alloy steels used in offshore applications [31].	Reciprocating ball-on-disc tribometer	Ø 10 mm Al_2O_3 ball	49 N 23 °C and 2 °C	1 mV/s 2.5 Hz	Synthetic seawater Ag/AgCl, Platinum wire	They employed two different electrolyte temperatures for tribocorrosion testing. At 23 °C, the steels showed a greater COF during tribocorrosion tests. It was established that temperature significantly impacted the steel's tribocorrosion behaviour, as evidenced by the larger material losses attributable to corrosion at higher test temperatures.
Tribocorrosion behaviour of mooring high strength low alloy steels in synthetic seawater [142].	Ball-on-disc unidirectional tribometer	Ø 10 mm alumina ball	5 N RT	1 mV/s 100 rpm	Synthetic seawater Ag/AgCl, Platinum wire	The study revealed that the corrosion products and the applied potential significantly influence the friction coefficient of the steel. Under the selected testing conditions, the two steel grades exhibited a similar tribocorrosion behaviour in seawater.

Table 5. *Cont.*

Title and Reference(s)	Tribometer Configuration	Counter Body	Applied Load and Temperature	Scan Rate and Sliding Speed	Electrolyte and Electrode	Findings
Mechanical and electrochemical deterioration mechanisms in the tribocorrosion of Al alloys in NaCl and in $NaNO_3$ solutions [157].	Reciprocating ball-on-plate tribometer	Ø 6 mm alumina ball	1.3 and 4 N 22 °C	1 Hz, 11.4 mm/s	0.05 M NaCl and 0.1 $NaNO_3$ solutions SCE, Platinum wire	The investigation showed that wear rates in $NaNO_3$ solutions are somewhat lower than in NaCl. It was further discovered that wear-accelerated corrosion had a minimal contribution to the total degradation of the aluminium alloy, which was primarily controlled by mechanical wear.
Tribocorrosion and corrosion behavior of quaternary Ti-24Nb-xZr-ySn alloys in SBF [94].	Ball-on-flat reciprocating sliding configuration	Ø 10 mm alumina ball	1 N 37 °C	1 Hz	SBF + ion concentrations Calomel, Graphite bar	The study varied the composition of Zr. As a result, the alloy with a lower Zr composition showed better corrosion resistance, while those with a higher Zr composition depicted better resistance to mechanical contact. Further study on these properties is required to determine the suitability of the alloys as contact or static implant materials.
Bio-tribocorrosion resistance of CoB-Co2B and Co2B layers on CoCrMo alloy [158].	Linear reciprocating ball-on-flat tribometer	Ø 5 mm Al_2O_3 ball	20 N 15–30 °C	1 mV/s	Calf serum Ag/AgCl, Platinum wire	Their findings demonstrate how the cobalt boride layer can enhance the CoCrMo alloy's functionality and prolong its service life in biomedical applications.
Synergistic interactions between wear and corrosion of Ti-16Mo orthopedic alloy [42].	Ball-on-plate-tribometer	Ø 10 mm ZrO_2 ball	1.5 N 37 ± 0.5 °C	0.5 mV/s 1 Hz, 0.03 m/s	PBS SCE	Their findings show that the wear mechanism of Ti-16Mo alloy depends on the interplay between abrasion and adhesion. In their conclusion, Ti-16Mo alloy is a promising candidate for orthopaedic implant applications.
The effect of pH, fluoride and tribocorrosion on the surface properties of dental archwires [102].	reciprocal tribometer	Ø 6 mm Al_2O_3 ball	1 N 37 °C	0.5 and 1 mV/s	Artificial saliva SCE	Increased fluoride concentration in artificial saliva does not significantly affect the properties of NiTi alloy and stainless steel AISI 304. The positive hysteresis in the cyclic potentiodynamic curve showed susceptibility of NiTi to localised corrosion at the highest concentration studied. In contrast, the stainless steel dental archwire was found to be susceptible at smaller concentrations.
Tribo-corrosion and corrosion behaviour of titanium alloys with and without DLC films immersed in synthetic urine [159].	Reciprocating tribometer	Ø 4.76 mm Al_2O_3 ball	5 N	1 mV/s 1 Hz	Synthetic urine Ag/AgCl, Platinum wire	Their investigation, which compared 60NiTi, NiTi60T, and Ti–6Al–4V, found that 60NiTi alloy, without thermal treatment, is 70 times more susceptible to corrosion in the absence of DLC film. While the DLC coating enhanced the resistance to corrosion of the 60NiTi alloy and the Ti-6Al-4V alloy, the NiTi60T sample was significantly more susceptible to corrosion without DLC film.
Tribocorrosion of different biomaterials under reciprocating sliding conditions in artificial saliva [45].	Reciprocating sliding wear tester	Ø 10 mm ZrO_2 ball	3, 6, and 10 N 21 ± 2 °C	1 mV/s 3 and 6 Hz (0.012, 0.024 m/s)	Artificial saliva SCE, Platinum wire	The investigation focused on biomedical materials used in implants under different contact conditions. The data showed that the Co28Cr6Mo alloy had the lowest wear and friction, whereas the Nb specimen had poor tribological performance. Of the three specimens with the highest corrosion potential value, the cP-Ti specimen exhibited a more noble behaviour.
Tribocorrosion behavior of additive manufactured Ti-6Al-4V biomedical alloy [62].	Reciprocating ball-on-plate tribometer	Ø 10 mm Al_2O_3 ball	1 N 20 ± 2 °C	1 Hz	PBS fluid	The findings demonstrated that the microstructure and manufacturing processes used for the cast, hot pressing (HP), and laser engineered net shaping (LENS) Ti-6Al-4V alloys affect the tribocorrosion performance. Compared to the cast and HP samples, the LENS Ti-6Al-4V samples showed superior wear and corrosion resistance.

3.3.2. Future Perspectives

This review has shown that, while the frictional behaviour and the interaction between wear and corrosion in corrosive environments have been studied extensively, the role of the "third body" (wear debris or contaminants trapped in the sliding contact) has received less attention. Compared to the well-studied areas of lubrication and sliding wear, there is a lack of information on how various parameters influence the tribocorrosion of NiTi alloys [160–162]. To optimise the performance of NiTi-based alloys, it is crucial to investigate the underlying tribocorrosion processes, including the kinetics of passivation and repassivation. This highlights the need for a mechanistic model that considers the interlinked actions of sliding wear, electrochemical corrosion, passivation and repassivation, and other surface/morphological changes [123].

Understanding these synergistic interactions and mechanisms would allow accurate predictions of material loss due to the combined effects of wear and corrosion. Theoretical and/or empirical models can be employed for this purpose [163,164]. Incorporating theoretical modelling in this area has gained significant interest in recent decades. López-Ortega et al. [132] suggested developing models to predict material loss due to the synergistic effect of wear and corrosion. Similarly, Stack [165] and Blau et al. [166] emphasised the need to understand the performance and mechanisms of implants in medical applications. Guadalupe et al. [126] combined a tribological third body approach with a mechanical description to model tribocorrosion in a pressurised water reactor (PWR) environment. Their model provided a deeper understanding of the mechanisms involved and yielded quantitative predictions that agreed well with the experimental observations.

Corrosion is a vital component of a tribo-electrochemical system [123]. Simulating the corrosive testing environment requires considering the potential determined by the material's electrochemical properties and the concentration of oxidising agents [167]. A corresponding corrosion potential can be imposed on the metal using an external current source to simulate the effect of oxidising agents [164,168,169]. Electrochemical techniques like open circuit potential (OCP), potentiodynamic polarisation (PD), potentiostatic polarisation (PS), and electrochemical impedance spectroscopy allow researchers to vary corrosion conditions by adjusting the applied potential [57,137,170].

Bio-tribocorrosion, the deterioration of materials due to the combined effects of wear, corrosion, and biological interactions, is another under-investigated area. While Delgado-Brito et al. [158] and De Stefano et al. [4] explored bio-tribocorrosion in medical applications due to contact with body fluids, this aspect needs to be addressed in engineering applications. Understanding bio-tribocorrosion is crucial, especially considering microbial interactions in marine and offshore environments.

4. Conclusions

This study provides an overview of current trends in NiTi alloy with regard to corrosion and wear synergy in engineering and medical applications. This follows the gradual surface deterioration of metals and biomaterials due to tribocorrosion, which has posed a significant challenge to the lifespan of materials and inadvertently affects the efficiency of various load-bearing operations/applications. Understanding the synergy between the sliding wear and electrochemical measurements provides a promising approach to investigating the mechanisms, passivation kinetics, and parametric effects on the tribocorrosion process. In this study, the complexities of tribocorrosion, which often is influenced by several parameters (mechanical and corrosion) coupled with the lack of an integrated/efficient test system, have been highlighted. Also, the behaviour of NiTiNOL60 alloy and its interactions in different corrosive media and the wear mechanisms under the synergistic tribo-electrochemical testing conditions, as well as the individual sliding wear and corrosion activities, have been revealed in this study. This review has contributed to the literature and is expected to serve as a guide to researchers while designing tribocorrosion experiments and/or improving on an already existing study.

Author Contributions: Conceptualisation, A.O.O. and M.R.; methodology, A.O.O., A.N., C.-P.J. and M.R.; investigation, A.O.O., A.N., C.-P.J. and M.R.; writing—original draft preparation, A.O.O.; writing—review and editing, A.O.O., A.N., C.-P.J. and M.R.; supervision, A.N. and M.R.; project administration, A.O.O.; funding acquisition, M.R. All authors have read and agreed to the published version of the manuscript.

Funding: This research received no external funding.

Conflicts of Interest: The authors declare no conflicts of interest.

References

1. Totolin, V.; Pejaković, V.; Csanyi, T.; Hekele, O.; Huber, M.; Ripoll, M.R. Surface engineering of Ti6Al4V surfaces for enhanced tribocorrosion performance in artificial seawater. *Mater. Des.* **2016**, *104*, 10–18. [CrossRef]
2. Wood, R.J.K.; Lu, P. Coatings and Surface Modification of Alloys for Tribo-Corrosion Applications. *Coatings* **2024**, *14*, 99. [CrossRef]
3. Wood, R.J.K. Tribo-corrosion of coatings: A review. *J. Phys. D Appl. Phys.* **2007**, *40*, 5502–5521. [CrossRef]
4. De Stefano, M.; Aliberti, S.M.; Ruggiero, A. (Bio)Tribocorrosion in dental implants: Principles and techniques of investigation. *Appl. Sci.* **2022**, *12*, 7421. [CrossRef]
5. Okoani, A.O.; Nand, A.; Ramezani, M. Comparative Study of the Tribocorrosion Performance of NiTiNOL60 in Acidic, Alkaline, and Saline Environments. *J. Mater. Eng. Perform.* **2024**. [CrossRef]
6. Mischler, S.; Munoz, A.I. Tribocorrosion. In *Encyclopedia of Interfacial Chemistry*; Wandelt, K., Ed.; Elsevier: Oxford, UK, 2018; pp. 504–514. ISBN 978-0-12-809894-3.
7. Munoz, A.I.; Espallargas, N.; Mischler, S. Chapter 4—Tribocorrosion phenomena and concepts. In *Tribocorrosion*; AMunoz, I., Espallargas, N., Mischler, S., Eds.; Springer Briefs in Applied Sciences and Technology; Springer: Cham, Switzerland, 2020; pp. 35–42. ISBN 978-3-030-48107-0.
8. Munoz, A.I.; Espallargas, N.; Mischler, S. *Tribocorrosion*; Springer Briefs in Applied Sciences and Technology; Springer: Cham, Switzerland, 2020.
9. Miller, C.; DellaCorte, C.; Zou, M. Nanomechanical properties of hardened 60NiTi. *Mater. Sci. Eng. A* **2021**, *800*, 14028. [CrossRef]
10. Cheng, K.-Y.; Bijukumar, D.; Runa, M.; McNallan, M.; Mathew, M. Chapter 5—Tribocorrosion aspects of implant coatings: Hip replacements. In *Tribocorrosion: Fundamentals, Methods, and Materials*; Siddaiah, A., Ramachandran, R., Menezes, P.L., Eds.; Academic Press: Cambridge, MA, USA, 2021; pp. 93–126. ISBN 978-0-12-818916-0.
11. DellaCorte, C.; Wozniak, W.A. Design and manufacturing considerations for shockproof and corrosion-immune superelastic nickel-titanium bearings for a space station application. In Proceedings of the 41st Aerospace Mechanisms Symposium, Pasadena, CA, USA, 16–18 May 2012; NASA/TM-2012-216015. pp. 411–503.
12. Siddaiah, A.; Kasar, A.; Ramachandran, R.; Menezes, P.L. Chapter 1—Introduction to tribocorrosion. In *Tribocorrosion: Fundamentals, Methods, and Materials*; Siddaiah, A., Ramachandran, R., Menezes, P.L., Eds.; Academic Press: Cambridge, MA, USA, 2021; pp. 1–16. ISBN 978-0-12-818916-0.
13. Koch, G.; Varney, J.; Thompson, N.; Moghissi, O.; Gould, M.; Payer, J. *International Measures of Prevention, Application, and Economics of Corrosion Technologies Study*; Jacobson, G., Ed.; NACE international: Houston, TX, USA, 2016; pp. 1–216.
14. Zou, J.; Wang, Z.; Ma, Y.; Tan, L. Tribocorrosion Behavior and Degradation Mechanism of 316L Stainless Steel in Alkaline Solution: Effect of Tribo-Film. *Acta Metall. Sin. (Engl. Lett.)* **2022**, *35*, 1365–1375. [CrossRef]
15. Tan, L.; Wang, Z.; Ma, Y. Tribocorrosion Behavior and Degradation Mechanism of 316L Stainless Steel in Typical Corrosive Media. *Acta Metall. Sin. (Engl. Lett.)* **2021**, *34*, 813–824. [CrossRef]
16. Sun, Y.; Rana, V. Tribocorrosion behaviour of AISI 304 stainless steel in 0.5 M NaCl solution. *Mater. Chem. Phys.* **2011**, *129*, 138–147. [CrossRef]
17. Perrut, M.; Caron, P.; Thomas, M.; Couret, A. High temperature materials for aerospace applications: Ni-based superalloys and γ-TiAl alloys. *Comptes Rendus Phys.* **2018**, *19*, 657–671. [CrossRef]
18. Chen, X.; Guo, A.; Wang, J.; Lu, S.; Fu, T. Temperature dependence of tribological properties in NiTi shape memory alloy: A nanoscratching study. *Tribol. Int.* **2024**, *197*, 109812. [CrossRef]
19. Choi, H.; Roy, S. Investigating the effect of operating temperature on the tribo-mechanical behavior of cold rolled superelastic nickel titanium alloy. *Wear* **2023**, *523*, 204729. [CrossRef]
20. Ponthiaux, P.; Wenger, F.; Celis, J.-P. Tribocorrosion: Material behavior under combined conditions of corrosion and mechanical loading. In *Corrosion Resistance*; InTech: Hong Kong, China, 2012; pp. 81–106. ISBN 9535104675.
21. Kosec, T.; Močnik, P.; Legat, A. The tribocorrosion behaviour of NiTi alloy. *Appl. Surf. Sci.* **2014**, *288*, 727–735. [CrossRef]
22. Johnsen, R.; Von Der Ohe, C.B. Chapter 16—Tribocorrosion in marine environments. In *Tribocorrosion of Passive Metals and Coatings*; Landolt, D., Mischler, S., Eds.; Woodhead Publishing: Sawston, UK, 2011; pp. 441–474. ISBN 978-1-84569-966-6.
23. Wood, R.J.K. Marine wear and tribocorrosion. *Wear* **2017**, *376–377*, 893–910. [CrossRef]
24. Mathew, M.T.; Wimmer, M.A. Tribocorrosion in artificial joints: In vitro testing and clinical implications. In *Bio-Tribocorrosion in Biomaterials and Medical Implants*; Woodhead Publishing Series in Biomaterials; Woodhead Publishing: Sawston, UK, 2013; pp. 341–371.
25. Chen, Q.; Thouas, G.A. Metallic implant biomaterials. *Mater. Sci. Eng. R Rep.* **2015**, *87*, 1–57. [CrossRef]

26. Cao, S.; Mischler, S. Tribocorrosion of a CoCrMo alloy in sulfuric acid–Glycerol mixtures. *Wear* **2020**, *458–459*, 203443. [CrossRef]
27. Primozic, J.; Hren, M.; Mezeg, U.; Legat, A. Tribocorrosion Susceptibility and Mechanical Characteristics of As-Received and Long-Term In-Vivo Aged Nickel-Titanium and Stainless-Steel Archwires. *Materials* **2022**, *15*, 1427. [CrossRef]
28. Takadoum, J. Review on Corrosion, Tribocorrosion and Osseointegration of Titanium Alloys as Biomaterials. *Corros. Mater. Degrad.* **2023**, *4*, 644–658. [CrossRef]
29. Silva, R.C.C.; Nogueira, R.P.; Bastos, I.N. Tribocorrosion of UNS S32750 in chloride medium: Effect of the load level. *Electrochim. Acta* **2011**, *56*, 8839–8845. [CrossRef]
30. Attarzadeh, N.; Molaei, M.; Babaei, K.; Fattah-alhosseini, A. New promising ceramic coatings for corrosion and wear protection of steels: A review. *Surf. Interfaces* **2021**, *23*, 100997. [CrossRef]
31. López-Ortega, A.; Bayón, R.; Arana, J.L.; Arredondo, A.; Igartua, A. Influence of temperature on the corrosion and tribocorrosion behaviour of high-strength low-alloy steels used in offshore applications. *Tribol. Int.* **2018**, *121*, 341–352. [CrossRef]
32. Shabalovskaya, S.; Anderegg, J.; Van Humbeeck, J. Critical overview of Nitinol surfaces and their modifications for medical applications. *Acta Biomater.* **2008**, *4*, 447–467. [CrossRef] [PubMed]
33. Bayón, R.; Igartua, A.; González, J.J.; de Gopegui, U.R. Influence of the carbon content on the corrosion and tribocorrosion performance of Ti-DLC coatings for biomedical alloys. *Tribol. Int.* **2015**, *88*, 115–125. [CrossRef]
34. Chenglong, Y.; Dejun, K. Microstructure, Tribocorrosion and Corrosion Performances of Laser Cladded Ni625-xTiC Coatings in 3.5% NaCl Solution. *J. Therm. Spray Technol.* **2024**, *33*, 260–274. [CrossRef]
35. Skjöldebrand, C.; Tipper, J.L.; Hatto, P.; Bryant, M.; Hall, R.M.; Persson, C. Current status and future potential of wear-resistant coatings and articulating surfaces for hip and knee implants. *Mater. Today Bio* **2022**, *15*, 100270. [CrossRef] [PubMed]
36. Yan, C.; Zhang, Y.; Zeng, Q.; Zhu, X.; Tong, Z.; Feng, X. Comparative investigation on the tribocorrosion resistance of Ti6Al4V and 60NiTi alloys inimulated seawater environment. *Wear* **2024**, *550–551*, 205423. [CrossRef]
37. Alhamad, M.; Barão, V.A.R.; Sukotjo, C.; Cooper, L.F.; Mathew, M.T. Ti-Ions and/or Particles in Saliva Potentially Aggravate Dental Implant Corrosion. *Materials* **2021**, *14*, 5733. [CrossRef]
38. Chouhan, A.; Mungse, H.P.; Khatri, O.P. Surface chemistry of graphene and graphene oxide: A versatile route for their dispersion and tribological applications. *Adv. Colloid Interface Sci.* **2020**, *283*, 102215. [CrossRef] [PubMed]
39. Kumar, S.S.A.; Bashir, S.; Ramesh, K.; Ramesh, S. New perspectives on Graphene/Graphene oxide based polymer nanocomposites for corrosion applications: The relevance of the Graphene/Polymer barrier coatings. *Prog. Org. Coat.* **2021**, *154*, 106215. [CrossRef]
40. Zuo, Y.; Li, T.; Yu, P.; Zhao, Z.; Chen, X.; Zhang, Y.; Chen, F. Effect of graphene oxide additive on tribocorrosion behavior of MAO coatings prepared on Ti6Al4V alloy. *Appl. Surf. Sci.* **2019**, *480*, 26–34. [CrossRef]
41. Acar, M.T.; Kovacı, H.; Çelik, A. Investigation of corrosion and tribocorrosion behavior of boron doped and graphene oxide doped TiO_2 nanotubes produced on Cp-Ti. *Mater. Today Commun.* **2022**, *32*, 104182. [CrossRef]
42. Xu, W.; Yu, A.; Lu, X.; Tamaddon, M.; Ng, L.; Hayat, M.D.; Wang, M.; Zhang, J.; Qu, X.; Liu, C. Synergistic interactions between wear and corrosion of Ti-16Mo orthopedic alloy. *J. Mater. Res. Technol.* **2020**, *9*, 9996–10003. [CrossRef]
43. Landolt, D.; Mischler, S. *Tribocorrosion of Passive Metals and Coatings*; Elsevier: Amsterdam, The Netherlands, 2011.
44. Shahini, M.H.; Mohammadloo, H.E.; Ramezanzadeh, B. Recent approaches to limit the tribocorrosion of biomaterials: A review. *Biomass Convers. Biorefinery* **2024**, *14*, 4369–4389. [CrossRef]
45. Vilhena, L.; Oppong, G.; Ramalho, A. Tribocorrosion of different biomaterials under reciprocating sliding conditions in artificial saliva. *Lubr. Sci.* **2019**, *31*, 364–380. [CrossRef]
46. Zhang, Z.; Dandu, R.S.B.; Klu, E.E.; Cai, W. A Review on Tribocorrosion Behavior of Aluminum Alloys: From Fundamental Mechanisms to Alloy Design Strategies. *Corros. Mater. Degrad.* **2023**, *4*, 594–622. [CrossRef]
47. Puthillam, U.; Selvam, R.E. Tribocorrosion in biomaterials and control techniques: A review. *Corros. Rev.* **2023**, *42*, 37–56. [CrossRef]
48. Huang, X.; Kang, N.; Coddet, P.; El Mansori, M. Effects of test temperature on the ball-on-slab wear behavior of nickel-titanium shape memory alloys fabricated by laser powder bed fusion. *Tribol. Int.* **2024**, *196*, 109666. [CrossRef]
49. Li, G.; Bao, J.; Yu, T.; Chen, M. An atomistic study of effects of temperature and Ni element on the phase transition and wear behavior of NiTi shape memory alloy. *Tribol. Int.* **2024**, *192*, 109309. [CrossRef]
50. Shahirnia, M.; Farhat, Z.; Jarjoura, G. Effects of temperature and loading rate on the deformation characteristics of superelastic TiNi shape memory alloys under localized compressive loads. *Mater. Sci. Eng. A* **2011**, *530*, 628–632. [CrossRef]
51. Patel, S.K.; Behera, A. Evolution of Phases and their Influence on Shape Memory Effect by Varying Sintering Parameters of NiTi Alloys. *Met. Mater. Int.* **2022**, *28*, 2691–2705. [CrossRef]
52. Bao, S.; Zhang, L.; Peng, H.; Fan, Q.; Wen, Y. Effects of heat treatment on martensitic transformation and wear resistance of as-cast 60NiTi alloy. *Mater. Res. Express* **2019**, *6*, 086573. [CrossRef]
53. Yan, C.; Zeng, Q.; Khanlari, K.; Zhu, X.; Wang, Z. Characterization of microstructure, grain distribution, and tribocorrosion properties of NiTi-based alloy. *J. Mater. Sci.* **2022**, *57*, 21237–21250. [CrossRef]
54. Kapoor, D. Nitinol for medical applications: A brief introduction to the properties and processing of nickel titanium shape memory alloys and their use in stents. *Johns. Matthey Technol. Rev.* **2017**, *61*, 66–76. [CrossRef]
55. Ayyagari, A.; Gwalani, B.; Banerjee, R.; Scharf, T.W.; Mukherjee, S.; Barthelemy, C. Reciprocating sliding wear behavior of high entropy alloys in dry and marine environments. *Mater. Chem. Phys.* **2018**, *210*, 162–169. [CrossRef]

56. Boyer, R.R.; Cotton, J.D.; Mohaghegh, M.; Schafrik, R.E. Materials considerations for aerospace applications. *MRS Bull.* **2015**, *40*, 1055–1066. [CrossRef]
57. Mathew, M.T.; Pai, P.S.; Pourzal, R.; Fischer, A.; Wimmer, M.A. Significance of tribocorrosion in biomedical applications: Overview and current status. *Adv. Tribol.* **2009**, *2009*, 250986. [CrossRef]
58. Shittu, J.; Sadeghilaridjani, M.; Pole, M.; Muskeri, S.; Ren, J.; Liu, Y.; Tahoun, I.; Arora, H.; Chen, W.; Dahotre, N.; et al. Tribo-corrosion response of additively manufactured high-entropy alloy. *NPJ Mater. Degrad.* **2021**, *5*, 31. [CrossRef]
59. Liu, M.; Zhu, J.-N.; Popovich, V.A.; Borisov, E.; Mol, J.M.C.; Gonzalez-Garcia, Y. Corrosion and passive film characteristics of 3D-printed NiTi shape memory alloys in artificial saliva. *Rare Met.* **2023**, *42*, 3114–3129. [CrossRef]
60. Buciumeanu, M.; Bagheri, A.; Silva, F.S.; Henriques, B.; Lasagni, A.F.; Shamsaei, N. Tribocorrosion behavior of NiTi biomedical alloy processed by an additive manufacturing laser beam directed energy deposition technique. *Materials* **2022**, *15*, 691. [CrossRef]
61. Grabarczyk, J.; Gaj, J.; Pazik, B.; Kaczorowski, W.; Januszewicz, B. Tribocorrosion behavior of Ti6Al4V alloy after thermo-chemical treatment and DLC deposition for biomedical applications. *Tribol. Int.* **2021**, *153*, 106560. [CrossRef]
62. Buciumeanu, M.; Bagheri, A.; Shamsaei, N.; Thompson, S.M.; Silva, F.S.; Henriques, B. Tribocorrosion behavior of additive manufactured Ti-6Al-4V biomedical alloy. *Tribol. Int.* **2018**, *119*, 381–388. [CrossRef]
63. Kaya, I.; Karaca, H.E.; Souri, M.; Chumlyakov, Y.; Kurkcu, H. Effects of orientation on the shape memory behavior of Ni 51 Ti 49 single crystals. *Mater. Sci. Eng. A* **2017**, *686*, 73–81. [CrossRef]
64. Halani, P.R.; Kaya, I.; Shin, Y.C.; Karaca, H.E. Phase transformation characteristics and mechanical characterization of nitinol synthesized by laser direct deposition. *Mater. Sci. Eng. A* **2013**, *559*, 836–843. [CrossRef]
65. Pješčić-Šćepanović, J.; Vastag, G.; Ivošević, Š.; Kovač, N.; Rudolf, R. Corrosion of NiTiDiscs in Different Seawater Environments. *Materials* **2022**, *15*, 2841. [CrossRef]
66. Dellacorte, C.; Pepper, S.V.; Noebe, R.; Hull, D.R. Nickel-titanium: A new candidate material for oil-lubricated bearing and mechanical component applications. In Proceedings of the World Tribology Congress 2009, Kyoto, Japan, 6–11 September 2009.
67. Buehler, W.J.; Wang, F.E. A summary of recent research on the nitinol alloys and their potential application in ocean engineering. *Ocean. Eng.* **1968**, *1*, 105–120. [CrossRef]
68. Dobrzański, L.A.; Dobrzański, L.B.; Dobrzańska-Danikiewicz, A.D.; Dobrzańska, J. Nitinol type alloys general characteristics and applications in endodontics. *Processes* **2022**, *10*, 101. [CrossRef]
69. Chen, W.; Xi, R.; Jiang, H.; Li, X.; Dong, G.; Wang, X. Superelasticity of Geometrically Graded NiTi Shape Memory Alloys. *Metals* **2023**, *13*, 1518. [CrossRef]
70. Du, Z.; Hu, Z.; Feng, Y.; Mo, F. The effect of powder composition on the microstructure and corrosion resistance of laser cladding 60NiTi alloy coatings on SS 316L. *Metals* **2021**, *11*, 1104. [CrossRef]
71. Stanford, M.K. Hot isostatic pressing of 60-Nitinol. In *NASA Technical Report*; NASA/TM-2015-218884; National Technical Information Service: Alexandria, VA, USA, 2015.
72. Li, M.-L.; Gao, W.-J.; Zhou, Y.-H. Hot deformation behavior of 60NiTi shape-memory alloy fabricated by hot isostatic pressing. *Mater. Res. Express* **2022**, *9*, 016511. [CrossRef]
73. Khanlari, K.; Shi, Q.; Li, K.; Hu, K.; Tan, C.; Zhang, W.; Cao, P.; Achouri, I.E.; Liu, X. Fabrication of ni-rich 58NiTi and 60NiTi from elementally blended Ni and Ti powders by a laser powder bed fusion technique: Their printing, homogenization and densification. *Int. J. Mol. Sci.* **2022**, *23*, 9495. [CrossRef]
74. Moskvichev, E.; Shamarin, N.; Savchenko, N. High temperature tribological properties of additively manufactured WC reinforced CuAl7-W composites. *Wear* **2024**, *556*, 205535. [CrossRef]
75. Ortiz, C.H.; Esguerra-Arce, A.; Esguerra-Arce, J.; Castañeda, A.B.; Caicedo, J.C.; Aguilar, Y. The high temperature tribological behavior of an iron oxide strengthened iron compound obtained from an industrial byproduct. *Tribol. Int.* **2022**, *175*, 107834. [CrossRef]
76. Okoani, A.O.; Nand, A.; Ramezani, M. Corrosion and wear interplay: Tribo-electrochemical evaluation of NiTiNOL60 alloy in sulfuric acid. *Results Mater.* **2024**, *21*, 100523. [CrossRef]
77. Pepper, S.V.; DellaCorte, C.; Noebe, R.D.; Hull, D.R.; Glennon, G. Nitinol 60 as a material for spacecraft triboelements. In Proceedings of the 13th European Space Mechanisms and Tribology Symposium-ESMATS 13 Conference, Vienna, Austria, 23–25 September 2009.
78. Atapour, M.; Wallinder, I.O.; Hedberg, Y.S. Stainless steel in simulated milk and whey protein solutions—Influence of grade on corrosion and metal release. *Electrochim. Acta* **2020**, *331*, 135428. [CrossRef]
79. Varmaziar, S.; Atapour, M.; Hedberg, Y.S. Corrosion and metal release characterization of stainless steel 316L weld zones in whey protein solution. *NPJ Mater. Degrad.* **2022**, *6*, 19. [CrossRef]
80. Jellesen, M.S.; Hansen, M.Ø.; Hilbert, L.R.; Møller, P. Corrosion and wear properties of materials used for minced meat production. *J. Food Process Eng.* **2009**, *32*, 463–477. [CrossRef]
81. Zaffora, A.; Franco, F.D.; Santamaría, M. Corrosion of stainless steel in food and pharmaceutical industry. *Curr. Opin. Electrochem.* **2021**, *29*, 100760. [CrossRef]
82. Wadood, A. Brief overview on NiTinol as biomaterial. *Adv. Mater. Sci. Eng.* **2016**, *2016*, 4173138. [CrossRef]
83. Khan, L.A.; McCarthy, E.; Muilwijk, C.; Ahad, I.U.; Brabazon, D. Analysis of NiTinol actuator response under controlled conductive heating regimes. *Results Eng.* **2023**, *18*, 101047. [CrossRef]

84. Xue, Y.; Hu, Y.; Wang, Z. Tribocorrosion behavior of NiTi alloy as orthopedic implants in Ringer's simulated body fluid. *Biomed. Phys. Eng. Express* **2019**, *5*, 045002. [CrossRef]
85. Zhu, X.; Dang, B.; Li, F.; Wei, D.; Zhang, P.; Li, S. Tribocorrosion behavior of Nb coating deposited by double-glow plasma alloying. *Mater. Res. Express* **2021**, *8*, 016411. [CrossRef]
86. Cao, S.; Maldonado, S.G.; Mischler, S. Tribocorrosion of passive metals in the mixed lubrication regime: Theoretical model and application to metal-on-metal artificial hip joints. *Wear* **2015**, *324–325*, 55–63. [CrossRef]
87. Minnath, M.A. Chapter-Metals and alloys for biomedical applications. In *Fundamental Biomaterials: Metals*; Woodhead Publishing: Duxford, UK, 2018; pp. 167–174. ISBN 9780081022054.
88. Geetha, M.; Singh, A.K.; Asokamani, R.; Gogia, A.K. Ti based biomaterials, the ultimate choice for orthopaedic implants–A review. *Prog. Mater. Sci.* **2009**, *54*, 397–425. [CrossRef]
89. Brantley, W.; Berzins, D.; Iijima, M.; Tufekçi, E.; Cai, Z. Chapter 1—Structure/property relationships in orthodontic alloys. In *Orthodontic Applications of Biomaterials*; Eliades, T., Brantley, W.A., Eds.; Woodhead Publishing: Sawston, UK, 2017; pp. 3–38. ISBN 978-0-08-100383-1.
90. Revathi, A.; Borrás, A.D.; Muñoz, A.I.; Richard, C.; Manivasagam, G. Degradation mechanisms and future challenges of titanium and its alloys for dental implant applications in oral environment. *Mater. Sci. Eng. C* **2017**, *76*, 1354–1368. [CrossRef]
91. Dong, H.; Liu, H.; Zhou, N.; Li, Q.; Yang, G.; Chen, L.; Mou, Y. Surface Modified Techniques and Emerging Functional Coating of Dental Implants. *Coatings* **2020**, *10*, 1012. [CrossRef]
92. Geringer, J.; Kim, K.; Boyer, B. *Chapter 14—Fretting corrosion in biomedical implants, In Tribocorrosion of Passive Metals and Coatings*; Landolt, D., Mischler, S., Eds.; Woodhead Publishing: Sawston, UK, 2011; pp. 401–423. ISBN 978-1-84569-966-6.
93. Waqar, S.; Wadood, A.; Mateen, A.; Rehman, M.A.U. Effects of Ni and Cr addition on the wear performance of NiTi alloy. *Int. J. Adv. Manuf. Technol.* **2020**, *108*, 625–634. [CrossRef]
94. Salas, L.; Chávez, J.; Jimenez, O.; Flores-Jimenez, M.; Alvarado-Hernandez, F.; Olmos, L.; Pérez-Alvarez, J.; Flores, M. Tribocorrosion and corrosion behavior of quaternary Ti-24Nb-xZr-ySn alloys in SBF. *Mater. Lett.* **2021**, *283*, 128903. [CrossRef]
95. Manam, N.S.; Harun, W.S.W.; Shri, D.N.A.; Ghani, S.A.C.; Kurniawan, T.; Ismail, M.H.; Ibrahim, M.H.I. Study of corrosion in biocompatible metals for implants: A review. *J. Alloys Compd.* **2017**, *701*, 698–715. [CrossRef]
96. Kosec, T.; Močnik, P.; Mezeg, U.; Legat, A.; Ovsenik, M.; Jenko, M.; Grant, J.T.; Primožič, J. Tribocorrosive study of new and in vivo exposed nickel titanium and stainless steel orthodontic archwires. *Coatings* **2020**, *10*, 230. [CrossRef]
97. Zupanc, J.; Vahdat-Pajouh, N.; Schäfer, E. New thermomechanically treated NiTi alloys–A review. *Int. Endod. J.* **2018**, *51*, 1088–1103. [CrossRef]
98. Ferreira, D.F.; Almeida, S.M.A.; Soares, R.B.; Juliani, L.; Bracarense, A.Q.; Lins, V.D.F.C.; Junqueira, R.M.R. Synergism between mechanical wear and corrosion on tribocorrosion of a titanium alloy in a Ringer solution. *J. Mater. Res. Technol.* **2019**, *8*, 1593–1600. [CrossRef]
99. Berradja, A.; Bratu, F.; Benea, L.; Willems, G.; Celis, J.P. Effect of sliding wear on tribocorrosion behaviour of stainless steels in a Ringer's solution. *Wear* **2006**, *261*, 987–993. [CrossRef]
100. Yan, C.; Zeng, Q.; He, W.; Zhu, J. Enhanced surface hardness and tribocorrosion performance of 60NiTi by boron ion implantation and post-annealing. *Tribol. Int.* **2021**, *155*, 106816. [CrossRef]
101. Kassab, E.; Gomes, J. Corrosion induced fracture of NiTi wires in simulated oral environments. *J. Mech. Behav. Biomed. Mater.* **2021**, *116*, 104323. [CrossRef] [PubMed]
102. Močnik, P.; Kosec, T.; Kovac, J.; Bizjak, M. The effect of pH, fluoride and tribocorrosion on the surface properties of dental archwires. *Mater. Sci. Eng. C Mater. Biol. Appl.* **2017**, *78*, 682–689. [CrossRef]
103. Močnik, P.; Kosec, T. A critical appraisal of the use and properties of nickel-titanium dental alloys. *Materials* **2021**, *14*, 7859. [CrossRef] [PubMed]
104. Costa, T.D.; Silva, E.; Caetano, P.L.; Campos, M.; Resende, L.M.; Machado, A.G.; Carmo, A.M.R.D. Corrosion resistance assessment of nickel-titanium endodontic files with and without heat treatment. *Restor. Dent. Endod.* **2021**, *46*, 6. [CrossRef]
105. Sifakakis, I.; Bourauel, C. Nickel–Titanium products in daily orthodontic practice. In *Orthodontic Applications of Biomaterials*; Eliades, T., Brantley, W.A., Eds.; Woodhead Publishing: Sawston, UK, 2017; pp. 107–127. ISBN 978-0-08-100383-1.
106. Romanos, G.E.; Fischer, G.A.; Delgado-Ruiz, R. Titanium wear of dental implants from placement, under loading and maintenance protocols. *Int. J. Mol. Sci.* **2021**, *22*, 1067. [CrossRef]
107. DellaCorte, C.; Noebe, R.D.; Stanford, M.K.; Padula, S.A. Resilient and Corrosion-Proof Rolling Element Bearings Made from Superelastic Ni-Ti Alloys for Aerospace Mechanism Applications. In *ASTM Special Technical Publication*; NASA/TM-2011-217105; NASA Center for Aerospace Information: Hanover, MD, USA, 2011; pp. 143–166.
108. Stanford, M.K. Preliminary investigation of surface treatments to enhance the wear resistance of 60-nitinol. In *NASA Technical Report*; NASA: Washington, DC, USA, 2016.
109. Benafan, O.; Garg, A.; Noebe, R.D.; Skorpenske, H.D.; An, K.; Schell, N. Deformation characteristics of the intermetallic alloy 60NiTi. *Intermetallics* **2017**, *82*, 40–52. [CrossRef]
110. Hornbuckle, B.C.; Yu, X.X.; Noebe, R.D.; Martens, R.; Weaver, M.L.; Thompson, G.B. Hardening behavior and phase decomposition in very Ni-rich Nitinol alloys. *Mater. Sci. Eng. A* **2015**, *639*, 336–344. [CrossRef]
111. DellaCorte, C. Nickel-Titanium alloys: Corrosion "proof" alloys for space bearing, components and mechanism applications. In Proceedings of the 40th Aerospace Mechanisms Symposium, Cocoa Beach, FL, USA, 12–14 May 2010; pp. 1–7.

112. DellaCorte, C. Novel super-elastic materials for advanced bearing applications. *Adv. Sci. Technol.* **2014**, *89*, 1–9.
113. Garcia-Cabezón, C.; Rodríguez-Méndez, M.L.; Borrás, V.A.; Bayón, R.; Salvo-Comino, C.; Garcia-Hernandez, C.; Martin-Pedrosa, F. Improvements in tribological and anticorrosion performance of porous Ti-6Al-4V via PEO coating. *Friction* **2021**, *9*, 1303–1318. [CrossRef]
114. Fotovvati, B.; Namdari, N.; Dehghanghadikolaei, A. On Coating Techniques for Surface Protection: A Review. *J. Manuf. Mater. Process.* **2019**, *3*, 28. [CrossRef]
115. Ramteke, S.M.; Walczak, M.; De Stefano, M.; Ruggiero, A.A. Rosenkranz, and M. Marian, 2D materials for Tribo-corrosion and -oxidation protection: A review. *Adv. Colloid Interface Sci.* **2024**, *331*, 103243. [CrossRef] [PubMed]
116. Rahmatian, B.; Ghasemi, H.M.; Sohi, M.H.; De Baets, P. Insight into tribocorrosion resistance and tribofilm formation on titanium boride coatings in a phosphate buffer saline solution. *J. Mater. Res. Technol.* **2023**, *27*, 6847–6862. [CrossRef]
117. Dong, J.; Zhang, Z.; Wang, D.; Liu, Y.; Wu, Y.; Guo, Y. Research on erosion wear behavior of NiTi alloy coating fabricated via high-frequency induction heating technology. *Wear* **2024**, *556–557*, 205506. [CrossRef]
118. Shen, Y.; Luo, J.; Liao, B.; Chen, L.; Zhang, X.; Zhao, Y.; Pang, P.; Zeng, X. Enhanced Anti-Tribocorrosion Performance of Ti-DLC Coatings Deposited by Filtered Cathodic Vacuum Arc with the Optimization of Bias Voltage. *Coatings* **2022**, *12*, 697. [CrossRef]
119. López-Ortega, A.; Arana, J.L.; Rodríguez, E.; Bayón, R. Corrosion, wear and tribocorrosion performance of a thermally sprayed aluminum coating modified by plasma electrolytic oxidation technique for offshore submerged components protection. *Corros. Sci.* **2018**, *143*, 258–280. [CrossRef]
120. Yi, Z.; Wang, X.; Li, W.; Qin, X.; Li, Y.; Wang, K.; Guo, Y.; Li, X.; Zhang, W.; Wang, Z. Interfacial friction at action: Interactions, regulation, and applications. *Friction* **2023**, *11*, 2153–2180. [CrossRef]
121. Hutchings, I.M. *Tribology: Friction and Wear of Engineering Materials*; Boca Raton: Edward Arnold—A division of Hoddr & Stoughton London; CRC Press: Boca Raton, FL, USA, 1992; ISBN 0-340-56184-X.
122. Hutchings, I.; Shipway, P. Chapter 5—Sliding wear. In *Tribology, 2nd ed*; Hutchings, I., Shipway, P., Eds.; Butterworth-Heinemann: Oxford, UK, 2017; pp. 107–164. ISBN 978-0-08-100910-9.
123. Krawiec, H.; Vignal, V. Stress/strain effects on electrochemical activity: Metallurgical/mechanical/interactions and surface reactivity. In *Mechanical and Electro-Chemical Interactions Under Tribocorrosion*; Ponthiaux, P., Celis, J.-P., Eds.; Woodhead Publishing: Sawston, UK, 2021; pp. 7–27. ISBN 978-0-12-823765-6.
124. Yang, J.; Song, Y.; Dong, K.; Han, E.-H. Research progress on the corrosion behavior of titanium alloys. *Corros. Rev.* **2023**, *41*, 5–20. [CrossRef]
125. Ghali, E. *Corrosion Resistance of Aluminum and Magnesium Alloys: Understanding, Performance, and Testing*; Wiley series in corrosion; John Wiley & Sons Inc.: Hoboken, NJ, USA, 2010; ISBN 978-0-471-71576-4.
126. Guadalupe, S.; Falcand, C.; Chitty, W.; Mischler, S. Tribocorrosion in pressurized high-temperature water: A mass flow model based on the third-body approach. *Tribol. Lett.* **2016**, *62*, 10. [CrossRef]
127. Perez, N. *Electrochemistry and Corrosion Science*; Kluwer Academic Publishers: New York, NY, USA, 2004; ISBN 978-1-402-07744-9.
128. Wellman, R.G. Chapter 9—Methods for studying erosion–corrosion. In *Tribocorrosion of Passive Metals and Coatings*; Landolt, D., Mischler, S., Eds.; Woodhead Publishing: Sawston, UK, 2011; pp. 239–264. ISBN 978-1-84569-966-6.
129. Azzi, M.; Klemberg-Sapieha, J.E. Chapter 8—Tribocorrosion test protocols for sliding contacts. In *Tribocorrosion of Passive Metals and Coatings*; Landolt, D., Mischler, S., Eds.; Woodhead Publishing: Sawston, UK, 2011; pp. 222–238. ISBN 978-1-84569-966-6.
130. Ponthiaux, P.; Wenger, F.; Drees, D.; Celis, J.P. Electrochemical techniques for studying tribocorrosion processes. *Wear* **2004**, *256*, 459–468. [CrossRef]
131. Jellesen, M.S.; Hansen, M.Ø.; Hilbert, L.R.; Møller, P. A block-on-ring tribocorrosion setup for combined electrochemical and friction testing. *Tribotest* **2007**, *13*, 115–127. [CrossRef]
132. López-Ortega, A.; Arana, J.L.; Bayón, R. Tribocorrosion of passive materials: A review on test procedures and standards. *Int. J. Corros.* **2018**, *2018*, 7345346. [CrossRef]
133. Mischler, S. Triboelectrochemical techniques and interpretation methods in tribocorrosion: A comparative evaluation. *Tribol. Int.* **2008**, *41*, 573–583. [CrossRef]
134. Munoz, A.I.; Espallargas, N.; Mischler, S. Chapter 6—Experimental techniques for tribocorrosion. In *Tribocorrosion*; Munoz, A.I., Espallargas, N., Mischler, S., Eds.; Springer Briefs in Applied Sciences and Technology; Springer: Cham: Switzerland, 2020; pp. 53–64. ISBN 978-3-030-48107-0.
135. Wang, X.Z.; Jiang, Y.; Wang, Y.; Ye, C.; Du, C.F. Probing the tribocorrosion behaviors of three nickel-based superalloys in sodium chloride solution. *Tribol. Int.* **2022**, *172*, 107581. [CrossRef]
136. Močnik, P.; Kosec, T. Tribo-corrosion properties of a NiTi dental wire. *Mater. Tehnol.* **2014**, *48*, 467–472.
137. Zhou, L.; Liu, H.; Yan, C.; Wei, Y.; Xia, Z.; Peng, H.; Tang, J. Electrochemical Behavior of Laser Powder Bed Fusion (L-PBF) Ti–6Al–4V Alloy: Influence of Phase and Grain Boundaries on Surface Passive Film Formation. *Met. Mater. Int.* **2024**, *30*, 1864–1877. [CrossRef]
138. Chen, J.; Yan, F.-Y. Tribocorrosion behaviors of Ti–6Al–4V and Monel K500 alloys sliding against 316 stainless steel in artificial seawater. *Trans. Nonferrous Met. Soc. China* **2012**, *22*, 1356–1365. [CrossRef]
139. Celis, J.P.; Ponthiaux, P.; Wenger, F. Tribo-corrosion of materials: Interplay between chemical, electrochemical, and mechanical reactivity of surfaces. *Wear* **2006**, *261*, 939–946. [CrossRef]

140. Muñoz, A.I.; Espallargas, N. Chapter 5—Tribocorrosion mechanisms in sliding contacts. In *Tribocorrosion of Passive Metals and Coatings*; Landolt, D., Mischler, S., Eds.; Woodhead Publishing: Sawston, UK, 2011; pp. 118–152. ISBN 978-1-84569-966-6.
141. Yan, C.; Zeng, Q.; Xu, Y.; He, W. Microstructure, phase and tribocorrosion behavior of 60NiTi alloy. *Appl. Surf. Sci.* **2019**, *498*, 143838. [CrossRef]
142. López, A.; Bayón, R.; Pagano, F.; Igartua, A.; Arredondo, A.; Arana, J.L.; González, J.J. Tribocorrosion behaviour of mooring high strength low alloy steels in synthetic seawater. *Wear* **2015**, *338–339*, 1–10. [CrossRef]
143. Qin, P.; Chen, L.Y.; Liu, Y.J.; Liang, S.X.; Sun, H.; Zhang, L.C. Corrosion and passivation behavior of laser powder bed fusion produced Ti-6Al-4V under various prior plastic deformation strains. *Corros. Sci.* **2024**, *230*, 111919. [CrossRef]
144. Zirari, T.; Trabadelo, V. A review on wear, corrosion, and wear-corrosion synergy of high entropy alloys. *Heliyon* **2024**, *10*, e25867. [CrossRef] [PubMed]
145. Uysal, I.; Yilmaz, B.; Atilla, A.O.; Evis, Z. Nickel titanium alloys as orthodontic archwires: A narrative review. *Eng. Sci. Technol. Int. J.* **2022**, *36*, 101277. [CrossRef]
146. Khanlari, K.; Ramezani, M.; Kelly, P. 60NiTi: A review of recent research findings, potential for structural and mechanical applications, and areas of continued investigations. *Trans. Indian Inst. Met.* **2018**, *71*, 781–799. [CrossRef]
147. Khanlari, K.; Ramezani, M.; Kelly, P.; Cao, P.; Neitzert, T. Reciprocating sliding wear behavior of 60NiTi as compared to 440C steel under lubricated and unlubricated conditions. *Tribol. Trans.* **2018**, *61*, 991–1002. [CrossRef]
148. Zeng, Q.; Dong, G. Superlubricity behaviors of Nitinol 60 alloy under oil lubrication. *Trans. Nonferrous Met. Soc. China* **2014**, *24*, 354–359. [CrossRef]
149. López-Ortega, A.; Bayón, R.; Arana, J.L. Evaluation of protective coatings for offshore applications. Corrosion and tribocorrosion behavior in synthetic seawater. *Surf. Coat. Technol.* **2018**, *349*, 1083–1097. [CrossRef]
150. Okoani, A.O.; Nand, A.; Ramezani, M. Tribocorrosion behaviour of NiTiNOL60 alloy in an alkaline environment. *Results Eng.* **2023**, *19*, 101305. [CrossRef]
151. Zhang, L.; Ren, D.; Ji, H.; Ma, A.; Daniel, E.F.; Li, S.; Jin, W.; Zheng, Y. Study on the corrosion behavior of NiTi shape memory alloys fabricated by electron beam melting. *NPJ Mater. Degrad.* **2022**, *6*, 79. [CrossRef]
152. Okoani, A.O.; Nand, A.; Ramezani, M. Tribo-electrochemical investigation of 60NiTi alloy in saline solution. *J. Alloys Metall. Syst.* **2024**, *6*, 100074. [CrossRef]
153. Chen, H.; Zhang, Z.; Hao, X.H.; Huang, B.X.; Zhao, X.C.; Hu, C.C. Microstructure and tribocorrosion properties of NiTi/AlNi2Ti ternary intermetallic alloy. *Vacuum* **2021**, *184*, 109928. [CrossRef]
154. Yu, Z.; Xu, Z.; Guo, Y.; Sha, P.; Liu, R.; Xin, R.; Li, L.; Chen, L.; Wang, X.; Zhang, Z.; et al. Analysis of microstructure, mechanical properties, wear characteristics and corrosion behavior of SLM-NiTi under different process parameters. *J. Manuf. Process.* **2022**, *75*, 637–650. [CrossRef]
155. Du, J.; Cao, S.; Munoz, A.I.; Mischler, S. Tribological and tribocorrosion behavior of nickel sliding against oxide ceramics. *Wear* **2019**, *426–427*, 1496–1506. [CrossRef]
156. Guadalupe, M.S.; Mischler, S.; Cantoni, M.; Chitty, W.J.; Falcand, C.; Hertz, D. Mechanical and chemical mechanisms in the tribocorrosion of a Stellite type alloy. *Wear* **2013**, *308*, 213–221. [CrossRef]
157. Vieira, A.C.; Rocha, L.A.; Papageorgiou, N.; Mischler, S. Mechanical and electrochemical deterioration mechanisms in the tribocorrosion of Al alloys in NaCl and in NaNO3 solutions. *Corros. Sci.* **2012**, *54*, 26–35. [CrossRef]
158. Delgado-Brito, A.; Mejía-Caballero, I.; Contla-Pacheco, A.; Pasten-Borja, R.P.; Castrejón-Sánchez, V.; Hernández-Ramírez, E.; Campos-Silva, I. Bio-tribocorrosion resistance of CoB–Co2B and Co2B layers on CoCrMo alloy. *J. Vac. Sci. Technol. A* **2024**, *42*, 023106. [CrossRef]
159. Paula, L.O.; Sene, A.C.; Manfroi, L.A.; Vieira, A.A.; Ramos, M.A.R.; Fukumasu, N.K.; Radi, P.A.; Vieira, L. Tribo-corrosion and corrosion behaviour of titanium alloys with and without DLC films immersed in synthetic urine. *J. Bio-Tribo-Corros.* **2018**, *4*, 51. [CrossRef]
160. Zeng, Q. Chapter 26—Superlubricity of NiTi alloys. In *Superlubricity*, 2nd ed.; Erdemir, A., Martin, J.M., Luo, J., Eds.; Elsevier: Amsterdam, The Netherlands, 2020; pp. 517–533. ISBN 9780444643131.
161. Zeng, Q.; Dong, G. Influence of load and sliding speed on super-low friction of NiTiNOL 60 alloy under castor oil lubrication. *Tribology Letters* **2013**, *52*, 47–55. [CrossRef]
162. Zeng, Q.; Dong, G.; Martin, J.M. Green superlubricity of Nitinol 60 alloy against steel in presence of castor oil. *Sci. Rep.* **2016**, *6*, 29992. [CrossRef] [PubMed]
163. Jiang, J.; Stack, M.M.; Neville, A. Modelling the tribo-corrosion interaction in aqueous sliding conditions. *Tribol. Int.* **2002**, *35*, 669–679. [CrossRef]
164. Olsson, C.-O.A.; Munoz, A.N.I.; Cao, S.; Mischler, S. Modeling current transients in a reciprocal motion tribocorrosion experiment. *J. Electrochem. Soc.* **2021**, *168*, 031503. [CrossRef]
165. Stack, M.M. Mapping tribo-corrosion processes in dry and in aqueous conditions: Some new directions for the new millennium. *Tribol. Int.* **2002**, *35*, 681–689. [CrossRef]
166. Blau, P.J.; Wood, R.; Stack, M.M.; Mischler, S.; Jiang, J.; Drees, D.; Rocha, L.A.; Wimmer, M.A.; Celis, J.P.; Cowan, R. Future needs and challenges in tribo-corrosion research and testing. In Proceedings of the Third International Symposium on Tribo-Corrosion, Atlanta, Georgia, 19–20 April 2013; ASTM Special Technical Publication 2013; STP 1563. pp. 214–226.

167. Kovač, N.; Ivošević, Š.; Vastag, G.; Vukelić, G.; Rudolf, R. Statistical approach to the analysis of the corrosive behaviour of NiTi alloys under the influence of different seawater environments. *Appl. Sci.* **2021**, *11*, 8825. [CrossRef]
168. Fallahnezhad, K.; Feyzi, M.; Ghadirinejad, K.; Hashemi, R.; Taylor, M. Finite element based simulation of tribocorrosion at the head-neck junction of hip implants. *Tribol. Int.* **2022**, *165*, 107284. [CrossRef]
169. von der Ohe, C.B.; Johnsen, R.; Espallargas, N. Modeling the multi-degradation mechanisms of combined tribocorrosion interacting with static and cyclic loaded surfaces of passive metals exposed to seawater. *Wear* **2010**, *269*, 607–616. [CrossRef]
170. Landolt, D.; Mischler, S.; Stemp, M. Electrochemical methods in tribocorrosion: A critical appraisal. *Electrochim. Acta* **2001**, *46*, 3913–3929. [CrossRef]